CHAPTER-1

INTRODUCTION

1.1 Metal oxide

Metal oxide are an interesting class of material intensively investigated nowadays , and displaying unique properties that include mechanical stress tolerance, high optical transparency, exceptional carrier mobilities etc. Metal oxides play a very important role in various areas of chemistry, physics, biology and materials science because of their interesting properties.

1.2. Materials Science

Materials science, which is also commonly known as materials science and engineering, is an interdisciplinary field dealing with the discovery and design of new materials. This relatively new scientific field involves the studies of materials through the materials paradigm (synthesis, structure, properties and performance). It incorporates elements of physics and chemistry and is at the forefront of nanoscience and nanotechnology research. In recent years, materials science has become more widely known as a specific field of science and engineering. A material is defined as a substance (most frequently a solid, but other condensed phases can be included) that is intended to be used for certain applications. There are many materials around us–they can be found in anything from buildings to spacecrafts. Materials can generally be divided into two classes: crystalline and non-crystalline. The traditional examples of materials are metals, ceramics and polymers. New and advanced materials that are being developed include semiconductors, nanomaterials, biomaterials etc. The

field has since broadened to include every class of materials like ceramics, polymers, semiconductors, magnetic materials, medical implant materials, biological materials and nanomaterials. Materials are so important in the development of civilization that we associate ages with them. In the origin of human life on earth, the Stone Age, people used only natural materials like stone, clay, skins and wood. Therefore, materials science is one of the most important multidisciplinary fields in science and engineering which is applied and utilizable science in day-to-day life.

- **Nanoscience**: The study of all kind of nanostructures, involving their properties and the processes that happen at nanometer scale (1 nm = 10^{-9} m).

- **Nanotechnology**: The search of the different applications of the studied nanostructures by trying to control and manipulate them.

1.3. Classifications of nanostructured materials (low dimensional systems)

In nanotechnology, the nanostructured materials are divided into different categories (Figure 1.1). The important method to classify nanostructured materials is their dimensionality. On the basis of the reduced dimensions to the nanoscale range (<100 nm), the nanostructured materials classified in the following categories:

- Zero dimensional (0-D) systems – In zero dimensional systems, all three dimensions (length, breadth and height) are in nanoscale level. In these systems, the charge carriers like electrons or holes are restricted in entire three dimensions and cannot move freely in any spatial direction. Zero dimensional systems include single crystal, polycrystalline and amorphous particles with all viable morphology similar to spheres, cubes and platelets. Example – Quantum dot.

- One dimensional (1-D) systems – In these systems, one dimension is in macroscale and other two dimensions are at nanoscale. The electrons or holes are free to move in one dimension and confined in other two dimensions. Example – Quantum wire.

- Two dimensional (2-D) systems – In these systems, two dimensions are in macroscale and one dimension is in nanoscale. The charge carriers are confined in one dimension and are free to move in two dimensions. Example – Quantum well.

- Three dimensional (3-D) systems – In these systems, all three dimensions are in macroscale and no dimensions are in nanoscale. In 3-D systems, charge carriers are free to move in every three dimensions. Example – Bulk material.

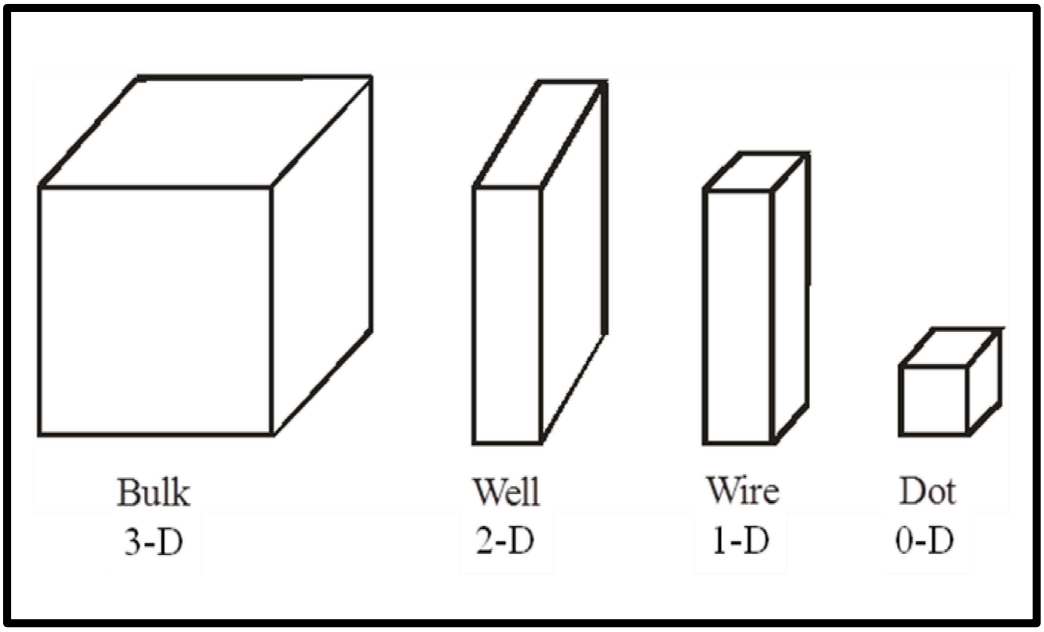

Figure 1.1. Schematic presentation of reduced-dimensional systems

Nanoparticles are defined as the particles that have at least one dimension in nano range (1 to 100 nm). These particles have high surface area and surface charge density which make them highly reactive. Nanoparticles act as a bridge between bulk materials and atomic or molecular structures [1]. The larger difference between these

two types of materials lies in the truth that bulk materials have constant physical properties regardless of its size, while nanostructures have size-dependent physical properties. For this reason, the properties of nanoparticles change as their size decreases and as the percentage of atoms at the surface of a material increases [2].

1.4. Metal oxides and mixed metal oxides nanoparticles

Among the various types of materials, metal oxides and mixed metal oxides are known for their different kinds of applications in human life. Metal oxides play a very important role in various areas of chemistry, physics, biology and materials science because of their interesting properties [3] [4], [5],. The metal elements are able to form a large diversity of oxide compounds by employing various synthesis methods . These can adopt an enormous number of structural geometries with an electronic structure that can exhibit metallic, semiconductor or insulator character. When two or more metal oxides are mixed together either by physical or by chemical methods to fabricate mixed metal oxide nanoparticles, a novel set of physical and chemical properties may be obtained that would be completely different from that of the individual constituents [6]. The distinct properties of nanomaterials arise from quantum size effects [7], quantum tunneling effects [8] and surface effects [9]. The confinement of carriers like electrons or holes in low dimensional systems or nanostructured materials could lead to a remarkable change in their physical and chemical properties due to the appearance of quantum size effects . The confinement or quantum size result becomes important when at least one dimension of the material is comparable to the de Broglie wavelength of the particle [10]. Physical properties of the materials at nanoscale size are predicted in expressions of quantum mechanics by Schrödinger wave equation which gives a quantitative understanding of different properties of nanostructured materials or low

dimensional systems. A low dimensional or confined system is any quantum system in which the charge carriers are free to move in one, two, or zero dimensions. In these systems, the spatial dimensions are of the order of the de Broglie wavelength of the carriers and thus the carrier energy states and density of states become quantized. Therefore the electrical, electronics, chemical, magnetic, and optical behavior of the carriers are governed by quantum-mechanical laws. These principles states that all matter at the nanoscale level behaves as both waves, and particles[11]. The complete information about a physical entity like electron, hole and photon or even a physical system such as an atom is explain by a wave function and is sufficient to show a particle or system of particles.

Nanomaterials (metal oxides and mixed metal oxides nanoparticles) have been synthesized in different morphologies, such as nanorods [12], nanowires[13], nanospheres [14], nanosheets , nanoplates , nanocubes [15], nanofibers [16] flower-like[17],[18]. [19], , hexagonal nanogranules, hierarchical nanostructures [20], nanoribbons[21], nanoflakes and nanotubes [22]. The physico-chemical properties of nanomaterials depend on the composition, particle size, surface area, shape, structure, crystallinity, homogeneity and synthetic methods [23], [24]. There are few examples like Ce_2O_3–TiO_2 composite nanofibers (Figure 1.2) [16], ZnO nanorings (Figure 1.3) , NiO nanotubes (Figure 1.4) [22], flower-like CuO (Figure 1. 5) and γ-Fe_2O_3 spherical nanoparticles (Figure 1. 6) [25].

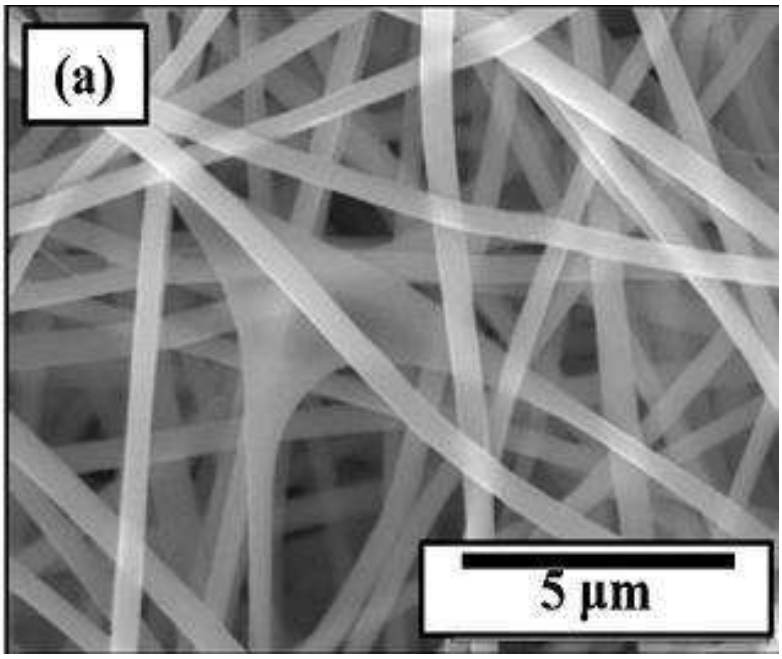

Figure 1.2. SEM image of the Ce_2O_3–TiO_2 composite nanofibers [M.S. Hassan et al. (2012)]

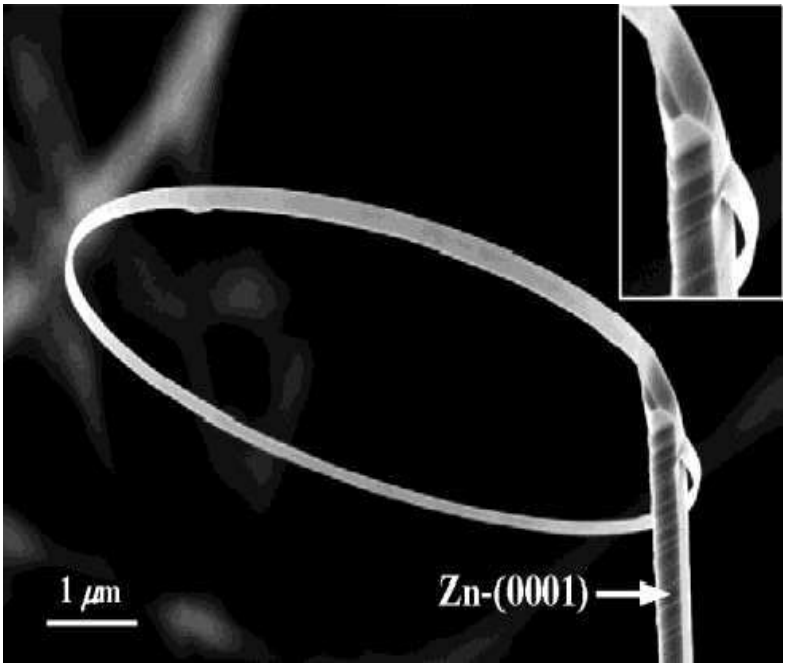

Figure 1.3. SEM image of ZnO nanorings .

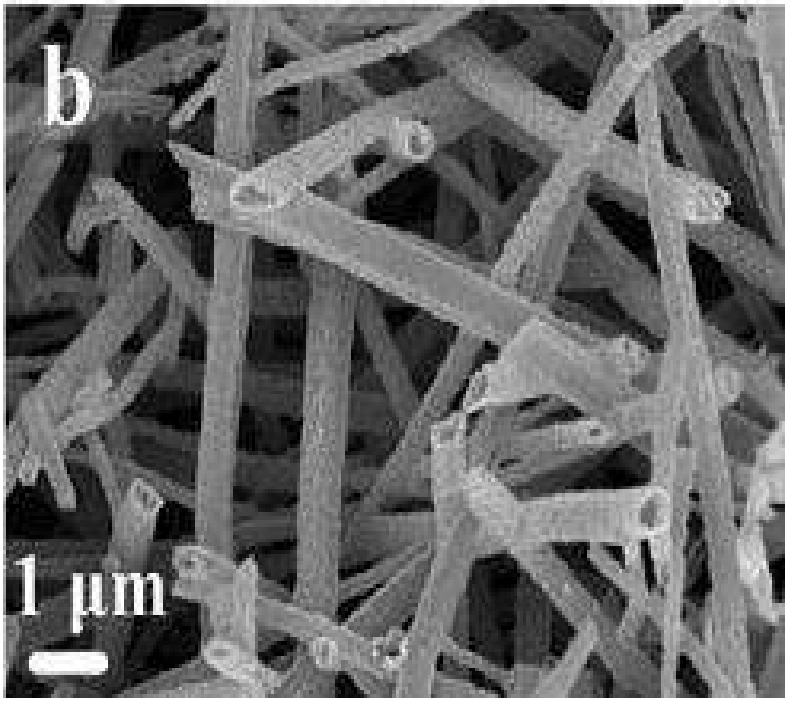

Figure 1.4. SEM image of NiO nanotubes .

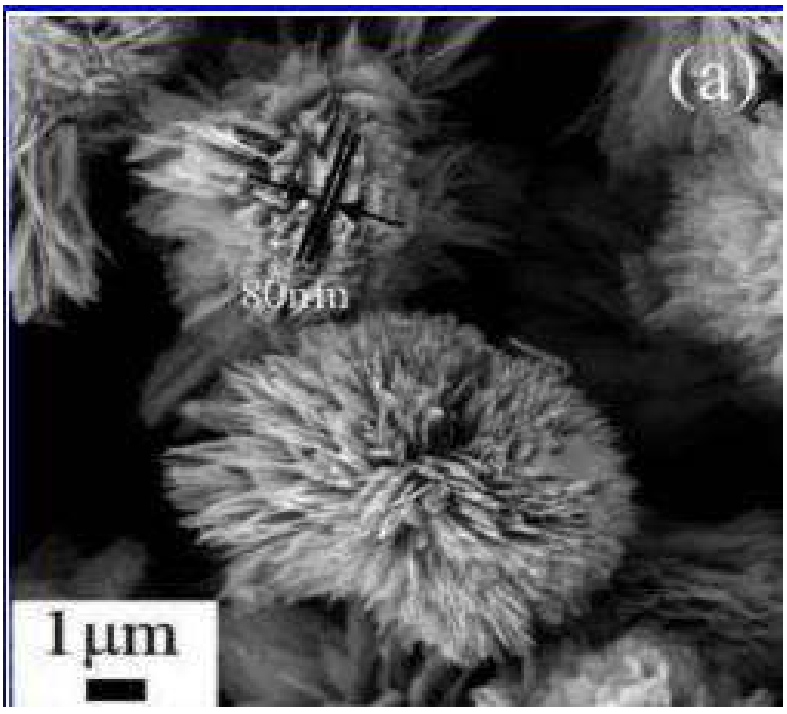

Figure 1.5. SEM image of flower-like CuO [M. Yang et al. (2011)]

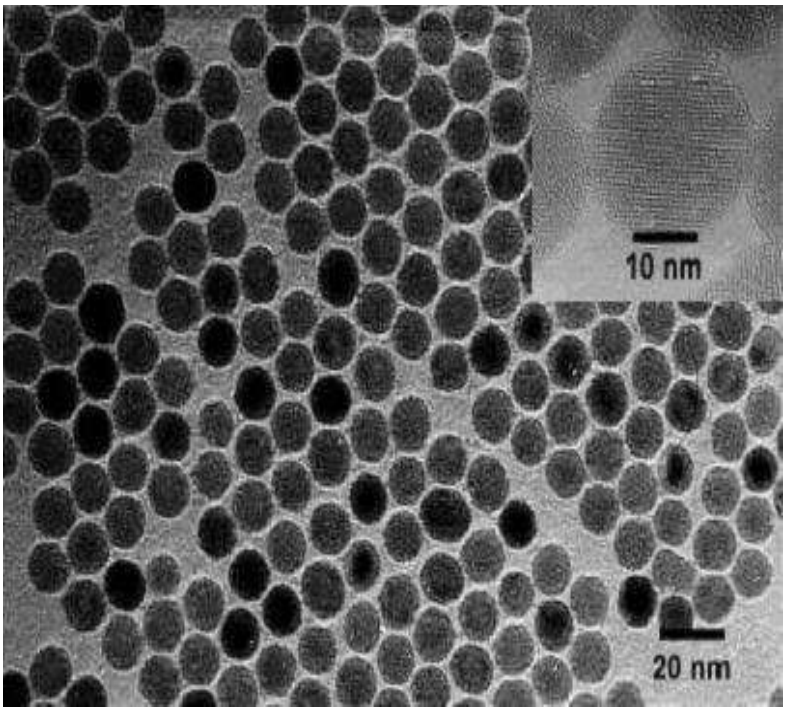

Figure 1.6. TEM image of γ-Fe_2O_3 spherical nanoparticles.[26]

1.5. Applications of metal oxides and mixed metal oxides nanoparticles

Metal oxides and mixed metal oxides nanoparticles have received extensive interest due to their potential uses in different applications, such as catalysis [19], photocatalysis [27] [28], sensors ,[19],[29] antimicrobial activity [30], [31] biomedical , electronics [32], optics[33] [33],[34],[35], magnetic materials [36], medicines[37], adsorbents [38],[39], UV-blockers and filters [40], fuels cells [41],[42][43], solar cells[44], waste water treatment ,[45] [23],[46],[47]] and ceramic materials [48] (Figure 1.7).

- Metal oxides and mixed metal oxides nanoparticles have also important applications in biological and medical sciences such as cancer treatments, drug delivery, fluorescent imaging, bio labeling and bio tagging .

- Gordon et al. have reported antibacterial activity of ZnO–Fe_2O_3 nanoparticles against *Escherichia coli* and *Staphylococcus aureus* [31].
- SnO_2–MgO nanoparticles perform as catalyst in different organic reactions, e.g. Baeyer–Villiger oxidation of cyclohexanone to caprolactone and oxidation of dimethyl ether to hydrocarbons[49].
- CuO–ZnO mixed oxide nanoparticles are active catalysts for CO oxidation at ambient temperature [50].
- Nanocrystalline MgO is used as an efficient adsorbent for many toxic chemicals (e. g. organophosphorous compounds) and acid gases[51],[52].
- SiO_2–NiO nanoparticles are considered as the best catalysts for the hydrogenation of benzene [53].
- ZnO nanoparticles exhibit strong antifungal activity against *Botrytis cinerea* and *Penicillium expansum* .
- TiO_2–ZnO mixed oxides are reported[54] as photocatalysts for hydrogen production from water splitting.
- NiO nanoparticles have a suitable adsorption capacity for the removal of heavy metals from aqueous solutions because of their high surface area, low production cost and natural porosity [55].
- Zinc oxide and titanium dioxide nanoparticles now appear on the ingredients list of general household products as various as cosmetics, toothpaste, sunscreens, food coloring, paint and coatings for vitamin supplements.

- $NiO/SrBi_2O_4$ photocatalytic disinfection of pathogenic bacteria Escherichia coli and Staphylococcus aureus in water under visible light irradiation [56].
- CuO–NiO nanoparticles have been used in humidity sensing.
- Hierarchical flower-like Co–Cu mixed metal oxide microspheres as highly efficient catalysts for selective oxidation of ethylbenzene.
- Nanostructures materials used in medicine, e.g. Active agents in cancer therapy and drug delivery, tissue engineering, fluorescent biological labels, fast test for medical diagnosis, detection of proteins, tumor destruction, separation and purification of biological molecules and cells.
- Nanostructures materials also used in cosmetics, e.g. Antiseptic cream, UV light protection creams and tooth paste.

These applications have resulted in a fast expansion of research in these kinds of structures. There is an enormous attention in the development of synthetic procedures in order to control shape, morphology, size and crystallinity of nanoparticles.

Figure 1.7. Application of metal oxides and mixed metal oxides nanoparticles in various fields

1.6 PEROVSKITE OXIDES: A GENERAL OVERVIEW

Since 1940, these oxides are a class of materials that have been extensively investigated, due to their significance to fundamental research and their high potential for technological applications including superconductivity, insulator–metal transition, ionic conduction characteristics, dielectric properties and ferroelectricity [57][58],[59] Perovskite play a very important role for chemical tuning of composition and structure and thus display of an over abundance of physical and chemical behaviors with

technological interest that depend on the processing conditions, oxygen content and ordering [60][61][62][63] and they are noticeable for their multitude of structure-dependent electronic, magnetic, optical and catalytic properties [64][65][66][67]. Their electrical properties range from insulators, semiconductors and some even exhibit metallic to superconductors characteristic[68][68],[69][70],[71].

The universal nature of the perovskite structure is the testament to its enormous structural and compositional suppleness. This suppleness allows perovskite oxides to be tuned to near an appropriate instability, be it structural, electronic, or magnetic in origin, which is essential for the oxide to be functionally useful [63],[72][73]. Titanate perovskite is a strong interest because of their thermoelectric and ferroelectric properties, their unusual electrochemical characteristics, and their industrial applications such as memories, transistors and electrodes. Alkaline earth metal titanate included $BaTiO_3$, $SrTiO_3$, $CaTiO_3$ and their associated non-stoichiometric complexes. (Ca, Sr, Ba) TiO_3, are important ferroelectric materials, which are the most extensively studied and widely utilized perovskite-type materials. $BaTiO_3$ is ferroelectric and $SrTiO_3$ and $CaTiO_3$ are quantum paraelectric. The structural suppleness of perovskite has been exhibited to produce or enhance desirable solid-state properties such as ionic or electronic conductivity [74]. The well known perovskite family is also the titanium-based oxides which are gaining more and more attention due to its promising applications in gas detection, nonlinear optics and so forth.

$CaTiO_3$ is widely used as a wireless device in electronic ceramic manufacturers and $BaTiO_3$ was a ferroelectric, piezoelectric, and an insulating material is widely used as high permittivity, low dielectric loss, and dielectric behaviors[75]. Whereas, $SrTiO_3$ was received much attention both theoretically and experimentally with respect to its defect chemistry and radiation resistance [76][77][78] Nowadays, the structural

properties of perovskite including order-disorder effects and formation of defects and impurities that can tailor the electronic and physico-chemical properties [79],[80][81]. The properties is these perovskite oxide may be modified to a novel system with completely unique characteristic. Over the last decade, extensive experimental and theoretical work on perovskite-based materials have demonstrated a strong inter relationship between distortions of the crystal structure and many processes and phenomena such as photoluminescence, ferroelectric, piezoelectric and pyroelectric properties [82],[83],[84][85].

1.7 Classification of Perovskite

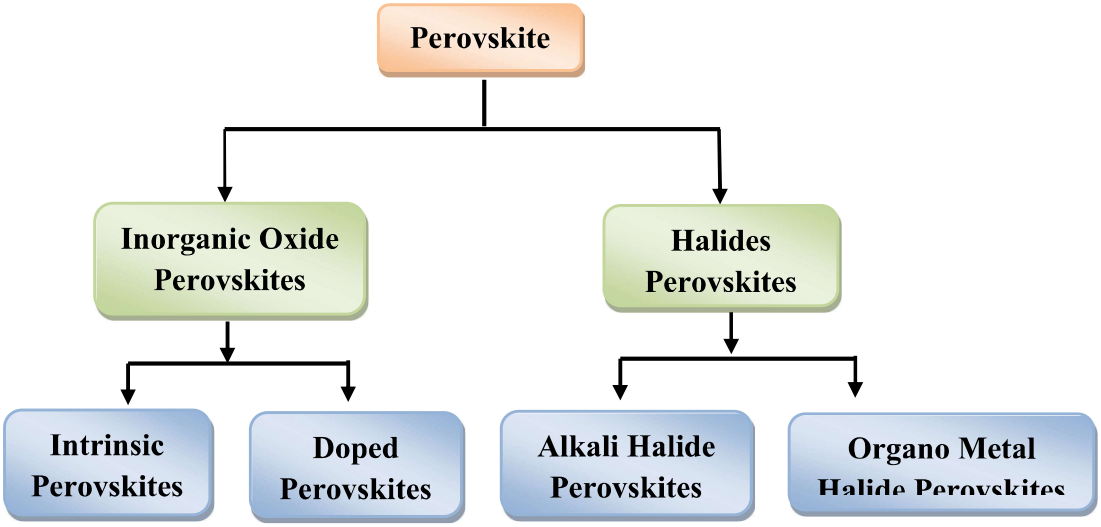

Fig.1.8. Classification of perovskite.

1.8 Type and Structures of Perovskite

a. **ABO_3 Perovskite:** The chemical formula of the perovskite structure is ABO_3, where A and B denote two different cations. It consists of BO_6 octahedral connected to each other by corner oxygen, and A cations occupy the 12-fold coordination sites surrounding eight BO_6 octahedral [85]. Therefore, the ionic radius of the A ion is larger than that of the B ion and the presence of two different size cation sites

enables a wide variety of perovskite-type oxides. Perovskite oxides always receives the much attention for their electrical and photo-catalysis properties[86],[87][88]and some example of perovskite used for ionic conductivity, ferromagnetic and piezoelectric i;e. $BaTiO_3$, $PdTiO_3$, $SrTiO_3$ and $CaTiO_3$ etc [89]. Perovskite also has structural suppleness regarding cation and anion vacancies. On the basis of this relationship, Goldschmidt proposed a tolerance factor (t), which represents a divergence from the ideal ratio of the ionic radii (equation 1.0).

$$t = \frac{r_A + r_O}{\sqrt{2} r_B + r_O} \qquad (1.0)$$

where r_A, r_B and r_O presenting ionic radaii of A, B and O ions respectively. The value of tolerance factor (t) is 1, its shows cubic structure but in case t < 1, A cation is too small to form a cubic structure, resulting in bends of the BO_6 octahedral network that reduces the space of the A cation site. Generally the range of perovskite compounds found to be 0:75 < t < 1 and cubic-type forms when t > 0:9.

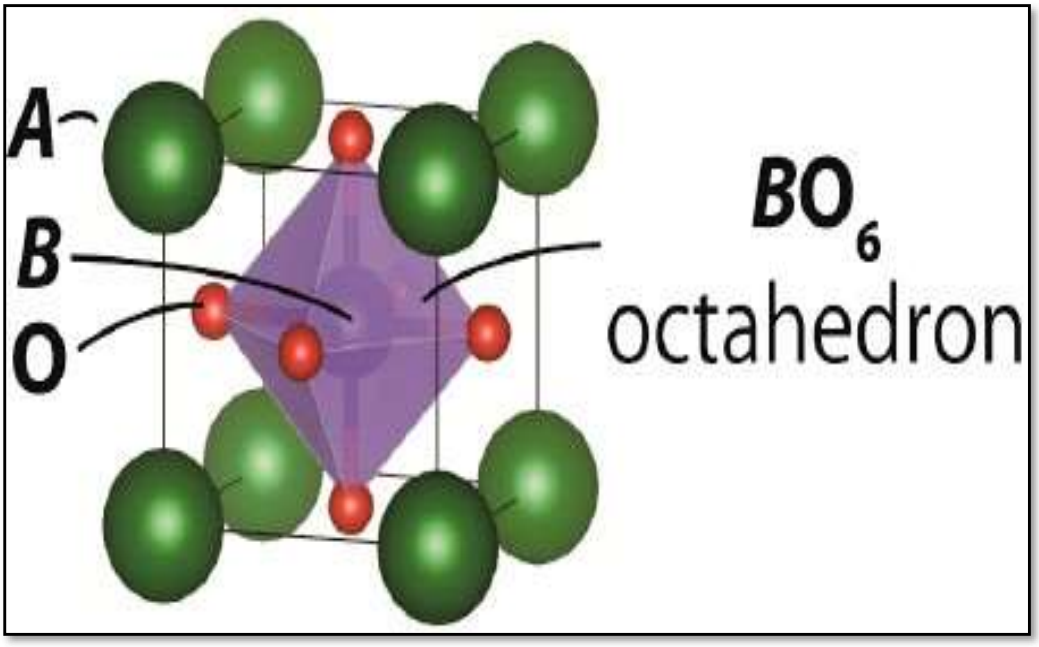

Fig.1.9. The structure of ABO_3 perovskite.[79]

b. **$A^{+1}B^{+5}O_3$ Perovskite:** $LiNbO_3$, $KNbO_3$, $AgNbO_3$, $NaNbO_3$ and $KNbO_3$ these are an example of $A^{+1}B^{+5}O_3$ of perovskite. Cation A belong to First group of element and cation B belong to the firth group element of the periodic table. These compound shows ferromagnetic and anti-ferromagnetic behavior [90]. Among these $NaNbO_3$ is an anti-ferromagnetic with the orthorhombic unit cell at room temperature but its change the structure at different- different temperature i.e; at 693 K pseudo-tetragonal, 833 K tetragonal and at 913 K its shows cubic structure. Mostly these perovskite compounds are widely used electro-optics devices.

c. **$A^{+2}B^{+4}O_3$ Perovskite:** $A^{+2}B^{+4}O_3$ type perovskite most widely used in dielectric and piezoelectric materials, A cation belongs to second groups and B cation belongs to the fourth group of the periodic table. Mostly A and B present to divalent (Ca, Sr and Ba) and tetravalent ion (Ti, Zr and Sn). Among these perovskite widely studied materials are $ATiO_3$, where A= Ba, Bi, Ca, La and Pb. It also used to dielectric and piezoelectric materials. Perovskite compound $BaTiO_3$ and $CaTiO_3$ materials useful for a large number of an application such as piezoelectric, transducers gas lighter elements, electronic ceramic materials and in immobilizing high-level radioactive waste [91].

d. **$A^{+3}B^{+3}O_3$ Perovskite:** This type of compounds belonging to rare earth or yttrium ion on A site and a trivalent transition metal ion on B site. The particular interest of these compounds found to be technical application of functional materials and most interest properties such as mixed conductivity by both ions and electron or hole migrations. Such materials can be employed in a solid electrolyte fuel cell (SOFC) as electrode materials for oxygen sensors and humidity sensors.

e. **$(ABO_3)_n$ AO Perovskite:** Ruddlesden and Popper have Mentioned a family of perovskite oxide with the general formula $A_{n+1}B_nO_{3n+1}$($(ABO_3)_nAO$), where, n is the number of ABO_3 perovskite layers separated by sole of AO rock salt layer [92]. A and B show the rare or alkaline earth elements. It belonging to R-P homologous series, and most of used for the high oxide-ionic conductivity, R–P homologous materials with mixed ionic electronic conductors for electrodes in intermediate temperature solid oxide fuel cells [93][94],[92]].

The interest of the R–P oxides as electrodes in intermediate temperature solid oxide fuel cells has been mainly focused on materials with a K_2NiF_4 like structure. K_2NiF_4 type materials present higher ionic conductivity than anion deficient ones due to the oxygen interstitial migration in the rock-salt type layers of the structure [95][96]. Besides, octahedral rotation distortions play an important role in the oxide–ion migration of these materials [97].

f. **$A_2B_2O_5$ Perovskite:** $A_2B_2O_5$ is the general formula for a large number of materials which exhibit an anion deficient perovskite (oxygen deficient perovskite) $ABO_{3-\delta}$ system. The brownmillerite considered the parent structure of $A_2B_2O_5$ ($A_2BB'O_5$) and giving rise to different derivatives, layered double perovskites, A site anion and anion vacancy ordered perovskites and perovskite oxide like compounds with crystallographic shear planes. Among anion deficient perovskites, $ABO_{2.5}$ (or $A_2B_2O_5$, $A_2BB'O_5$, and $AA'B_2O_5$, where A, A', B, and B' are cations of different kinds) are probably, the most popular and rich in a structural diversity. This type perovskite used high Curie temperature (T_c), superconductivity in Cu-based oxides, high electron and oxygen ion conductivity, and rich magnetic behavior, which makes them promising materials for different applications.

$Ca_2Mn_2O_5$ and $Ba_2In_2O_5$ are the best examples of the oxygen deficient perovskite. The orthorhombic structure of $Ca_2Mn_2O_5$ has five coordinated square pyramid subunits between manganese and oxygen, in which all five oxygen atoms are linked with adjacent subunits through corner oxygen atoms, as shown in figure 1.3.

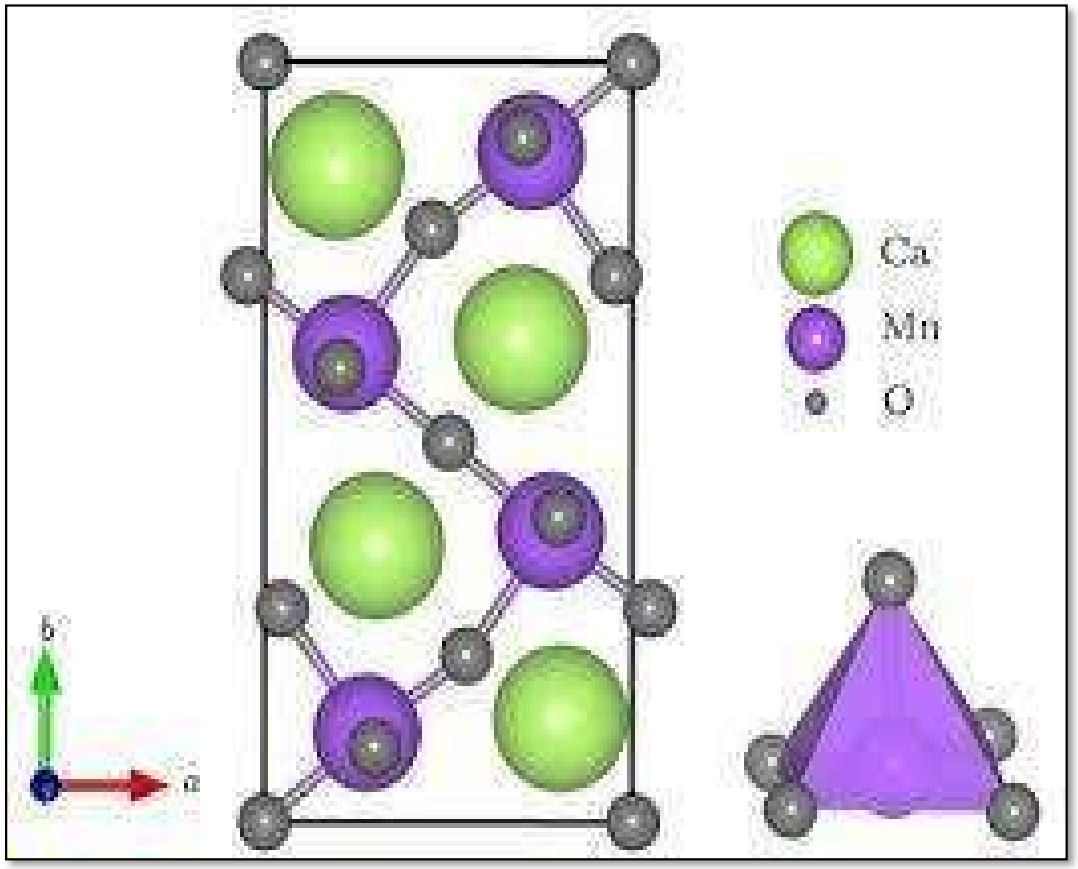

Fig.1.10.Structure of $Ca_2Mn_2O_5$ unit cell showing oxygen vacancy along the direction of normal A B plane.[98]

The orthorhombic $CaMnO_3$ has six-coordinated octahedral subunits linked through the six oxygen atoms at the corner sites. Thus, oxygen deficient perovskite $Ca_2Mn_2O_5$ has intrinsic molecular level porosity on the oxygen deficient sites, which are beyond structural porosity, such as mesoporosity or macro-porosity [85].

Table.1.1. Example of some perovskite explains property application and their use.

Compounds	Typical property	Application	Used
$BaTiO_3$, $PdTiO_3$	Ferromagnetic property Piezoelectricity and high dielectric constant.	Multilayer ceramic capacitors (MLCCs), PTCR resistors and embedded capacitance.	Most widely used dielectric ceramic T_C = 125°C
(Ba Sr)TiO_3, (Bi, Na)TiO_3	Non-Linear dielectric properties.	Tunable microwave devices.	Used in the para-electric state.
Pb(Zr, Ti)O_3	Ferromagnetic property Piezoelectricity.	Piezoelectric transducers actuators and ferroelectric memories.	PZT most successful piezoelectric material.
$Bi_4Ti_3O_{12}$	Ferroelectric with high Curie temperature.	High-temperature actuators and Ferroelectric Properties.	Aurivillius compound T_C = 675°C
$(K_{0.5}Na_{0.5})NbO_3$, $Na_{0.5}Bi_{0.5}TiO_3$	Ferromagnetic property Piezoelectricity.	Lead-free piezo-ceramics.	Performances not yet comparable to PZT but rapid progress.
$SrFeO_3$, $LaCoO_3$	Electrical conductivity.	Alternative dielectric materials and Internal barrier layer capacitors.	Multifunctional material.
$BiFeO_3$, $LaMnO_3$	Magnetic property.	Magnetic field detectors, Memories.	Most investigated multi ferroic compound. T_C = 850°C
$LaCoO_3$, $BaCuO_3$	Catalytic property.	Cathode material in SOFCs and oxygen separation membranes.	Used for Solid Oxide Fuel Cells cathodes.
$LaAlO_3$, $YAlO_3$	Host materials for rare-earth luminescent ions.	Lasers Substrates for epitaxial film deposition.	

1.9 Complex Perovskite

The complex perovskite $(A'A'')(B'B'')O_3$ type structure are well founded many technological applications due to configurational and compositional ductility of the perovskite octahedral texture. In these structure, cation A shows divalent species, although some compositions also consolidated trivalent rare earth, cation A with charge Indemnity conferred by the simultaneous consolidated of trivalent species like Al^{+3}, Ti^{+3}, and Fe^{+3} on the B site, for example $(Ca_{1-x}Nd_x)$ $(Ti_{1-x}Al_x)O_3$ and $(Pb_{1-x}Ba_x)$ $(Fe_{1-x}Ti_x)O_3$. A and B cations both are large difference in between size and charge, can also resulting in detractive of symmetry and changes the properties like that magnetic and dielectric behavior. The perovskite structure explains excellent latitude in chemical substitutions on both cations and therefore, a great deal over the control properties. The additional composition of perovskite A_3BX and BAX_3 inverse perovskite structure are belong to homologus series, such as $A_{n+1}B_nO_{3n+1}$ (Ruddlesden-Popper) [99][3], $A_nB_nO_{3n+1}$ (Dion-Jacobson)[100], $Bi_2A_{n-1}B_nO_{3n+3}$ (Aurivillius series) [B. Aurivillius (1949), B. Aurivillius (1950), B. Aurivillius (1951)]. The structures of some homologues series perovskite oxide explained anion deficient perovskite with many-sided properties like that $A_nB_nO_{3n-2}$ and its related to ABO_3 perovskite. Ruddlesden-Popper and Dion-Jacobson explained many application and properties of pervoskite i.e; ferroelectrics, ionic conductors, superconductors, multiferroic and magneto resistant materials result from a complex and interaction between the crystal structure, electronic state of the transition metal, amount of defects and their mutual interaction. $CaCu_3Ti_4O_{12}$ (CCTO), $Bi_{2/3}Cu_3Ti_4O_{12}$ (BCTO), $Y_{2/3}Cu_3Ti_4O_{12}$ (YCTO) and $La_{2/3}Cu_3Ti_4O_{12}$ (LCTO), are few example of complex perovskite oxide.

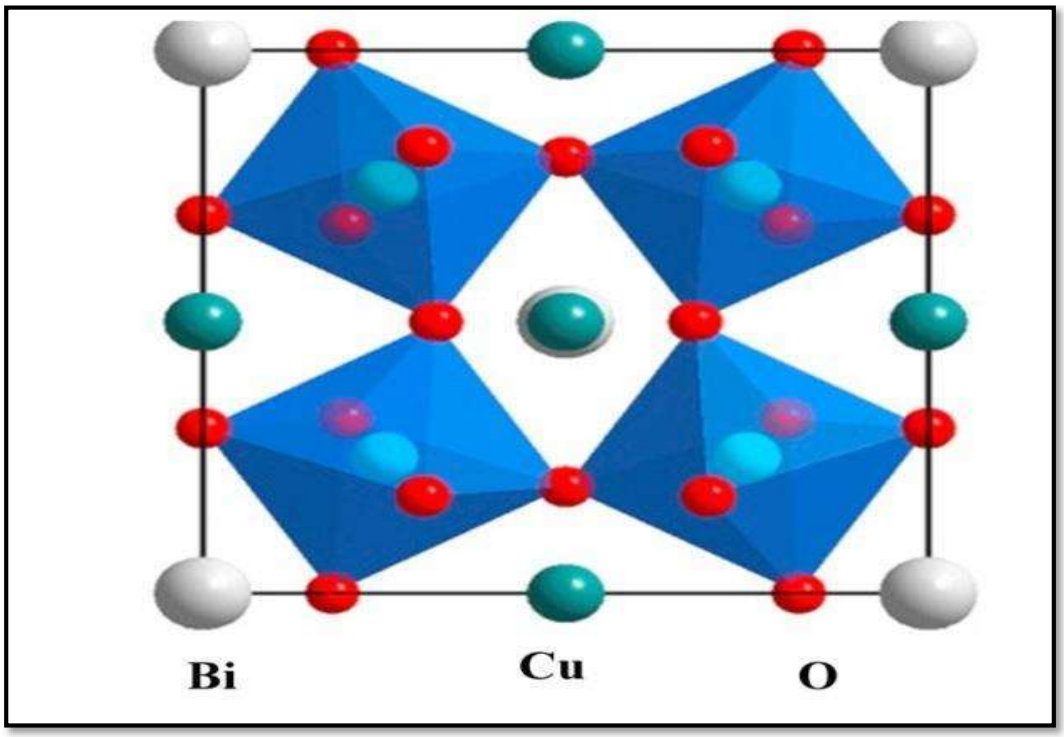

Fig.1.11. Crystal structure of $Bi_{2/3}Cu_3Ti_4O_{12}$ (BCTO)[101].

Fig.1.4. shows the cubic structure of $Bi_{2/3}Cu_3Ti_4O_{12}$ complex perovskite and their space group is Im3 and lattice constant a =7.413 Å. In this structure, the Bi sites are 1/3 vacant in order to achieve charge neutralism. This might affect the dielectric behavior, rendition the study of this compound more interesting. The Structure of BCTO similar to CCTO structure of complex perovskite.

1.10 History of Sillenite

Sillenite (i.e. stabilized γ-Bi_2O_3) was discovered in 1937 and named after L. G. Sillén, who accidently found a body-centred cubic phase by firing Bi_2O_3 with Al_2O_3 at 900 ºC for 5 minutes[102].

This phase was also obtained by Schumb and Rittner in 1943 by "fusing" Bi_2O_3 with SiO_2 at 875 ºC for 20 minutes. This phase was also obtained by Schumb and Rittner in 1943 by "fusing" Bi_2O_3 with SiO_2 at 875 ºC for 20 minutes. Aurivillius and

Sillén then noticed it was possible to stabilize γ- Bi_2O_3 at room temperature by using a small amount of various cations with ionic radii from 0.4 – 0.6 Å(11). Since then more than 60 sillenite members have been reported. Sillenites mention to a class of bismuth compounds with a structure similar to $Bi_{12}SiO_{20}$, whose parent structure is γ-Bi_2O_3, a meta-stable form of bismuth oxide[103].

The cubic crystal sillenite arrangement is pooled by several synthetic materials containing bismuth titanate and bismuth germanate. These compounds have been usually examined for their non-linear optical propertie.

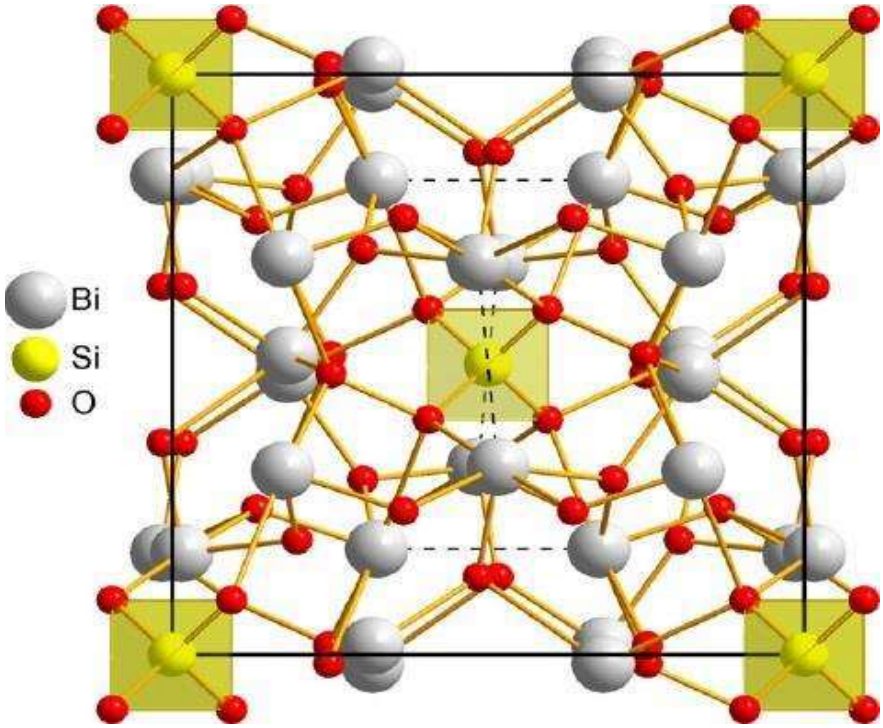

Figure.1.12. Crystal structure of the sillenite Bi_{12} SiO_{20} , space group I 23. The Bi^{3+} $6s^2$ lone electron pairs are oriented along the closest.[104]

The modern applications of sillenites are mainly in the fields of electrooptics, acoustics, and piezotechnics, where their physical properties such as photorefractivity,

optical activity, photoconductivity, piezo-modulus, the velocity of ultrasound wave propagation,1-3 etc., can be exploited. Recently, however, sillenites have begun to be considered for use as dielectrics in the field of electronics. 4 For the majority of these applications, the properties of the sillenites must be optimized or tuned to a certain value, and the adjustment of the properties to the requirements of a particular application demands a detailed understanding of the physics, the processing (crystal growth, film deposition, sintering, etc.), and the chemistry of the sillenites. The parent representative of the sillenites is γ-Bi_2O_3, a metastable compound that can be prepared only by controlled cooling. (13)[105] The crystal structure of γ-Bi_2O_3 has been the subject of a number of investigations that resulted in several different structural models.

All of the models have similar description of the structural framework that consists of the Bi-O coordination polyhedral. The Bi^{3+} ions within the framework are in octahedral coordination with the apical oxygen ion at a very short distance of ~2.05 Å, with the two basal-plane oxygen ions at ~2.2 Å, and with another two at ~2.6 Å.[6] The two oxygen ions from the adjacent octahedra are at a relatively long distance of ~3.1 Å from Bi^{3+} and are not usually considered as being part of the first coordination sphere. . Contradictory the apical oxygen, a stereochemically active $6s^2$ lone electron pair that completes the distorted octahedra spreads over a distance of ~1.8 Å. The Bi-O octahedra share corners to form the framework, within which the regular tetrahedral sites are occupied by M-site Bi ions. The structure and the tenancy of the M-site coordinational tetrahedra are the most disputed details of the γ-Bi_2O_3 crystal structure. Several authors have proposed several different solutions. Craig and Stephenson assumed a statistically alternating occupancy of the tetrahedral position by the Bi^{3+} and Bi^{5+} ions, with a fully occupied oxygen sublattice. This structural formula, which was the most broadly accepted structural model for a long time, should be written as

$Bi_{12}(Bi_{3+0.5}$- $Bi_{5+0.5})O_{20.}$ The model suffers from a major crystallographic discrepancy associated to the dimensions of the ions: it is highly unlikely that the large Bi^{3+} ion with its stereochemically active $6s^2$ lone electron pair can fit into the tetrahedral interstice[106]. Watanabe et al. 7 tried to avoid the tetrahedrally coordinated Bi^{3+} by suggesting a model in which the tetrahedral sites are fully occupied by the $Bi^{5+.}$ Because this model again assumes a fully occupied oxygen sublattice the charge compensation necessitates a deficiency in the Bi-O framework. . The structural formula should be written as $Bi^{3+}11.67Bi^{5+}O_{20}$. Unfortunately, a lack of experimental evidence for the presence of the Bi^{5+} ions has raised doubts about the validity of this model. In addition, the Bi^{5+} ion is destabilized at high temperatures and, therefore, not expected to exist in the high-temperature form of Bi_2O_3. Currently, many researchers (see, for example, refs 9-12) seem to agree that the structural model of Radaev and Simonov8 describes the γ-Bi_2O_3 crystal structure in such a way that it can explain all of the experimental observations. According to this model, the tetrahedral positions are 80% occupied by Bi^{3+} ions and 20% vacant. The Bi^{3+} ions are coordinated with three oxygen ions, and in the direction of the absent fourth oxygen, the $6s^2$ lone electron pair extends (identified as the [BiO_3] group). The vacant tetrahedral positions are regularly coordinated with four oxygen ions (to give the [0O4] group, where 0 is a vacancy) and statistically distributed over the lattice. The model assumes that the oxygen vacancies are due only to the presence of the [BiO_3] groups, which is reflected in the structural formula $Bi_{12}(Bi^{3+0.800.2})$O19.2(14). It should be mentioned that the work of Murray et al.,13 which preceded the study of Radaev and Simon8 and was performed on the isomorphous compound $Bi_{12}PbO_{19}$, already suggested the presence of [MO3] groups when the M ions exhibit a lone electron pair ([PbO_3] in the case of $Bi_{12}PbO_{19}$)[107]. In addition, for B3+ ions with a similar electronic configuration of the outer electron shell,

the possibility of forming [BO_3] groups has been demonstrated as well. The possibility of stabilizing metastable γ-Bi2O3 using a small amount of other cations has already been suggested by Sillen.[85]

1.11 Stoichiometric Sillenites

Whereas γ-Bi_2O_3 is considered stoichiometric despite having oxygen vacancies, Sillenites are only considered stoichiometric when they have a fully occupied oxygen lattice, i.e. a general formula of $Bi_{12}MO_{20}$. If Bi is (+III) and O is (-II), then in order to achieve a full oxygen lattice the M ion must be (+IV), such as Si^{4+}, Ge^{4+} or Ti^{4+} [107] However, it is also possible to produce Sillenites which simply have an average M-site charge of (+IV), such as $Bi_{12}(M^{3+}_{0.5}M^{5+})O_{20}$ [18] or $Bi_{12}(M^{5+})O_{20}$ [103].

1.12 Non-stoichiometric Sillenites

In a stoichiometric Sillenite the M-site should have an average charge of (+IV) but this can be changed by aliovalent substitution of the M site to produce non-stoichiometric Sillenites with a range of oxygen contents.

Valant's general structural model predicts a range of possibilities for forming oxygen deficient Sillenites by making the average M site charge less than (+IV) . Pentavalent ions can partially fill the M site, allowing a minimum oxygen content of 19.2. Also, (+III) ions can be substituted onto the M site. This is comparable to the case of γ-Bi_2except most commonly used (+III) ions such as Ga^{3+} or Fe^{3+} don't have an electron lone pair like Bi^{3+}. This means that unoccupied oxygen sites are then no longer filled by lone pairs. If the M site was fully occupied by a (+III) ion charge balance would predict an oxygen content of 19.5, leaving 0.5 oxygen sites completely vacant. In many cases it is postulated that the two are linked, with the M site occupying

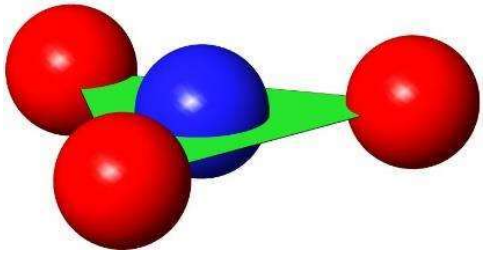

MO_3 trigonal sites like that shown in figure 1.13.

Figure 1.13: Trigonal coordination of an MO_3 group in an oxygen-deficient Sillenite.[108]

Oxygen-excess Sillenites are only possible by substitution of a (+V) ion such as V^{5+} or As^{5+} onto the M site [3]. It is theoretically possible to form oxygen-excess Sillenites using (+VI) ions, but the large positive charge of a (+VI) ion and the corresponding structural distortion this causes makes phase stability unlikely [12]. The structural position of the excess oxygen is not covered in the Valant and Suvorov model, it merely states that space is created by 'structural distortions'. Oxygen-excess Sillenites are better explained by the creation of an extra oxygen site, such as in the Radaev model.[79][34][108].

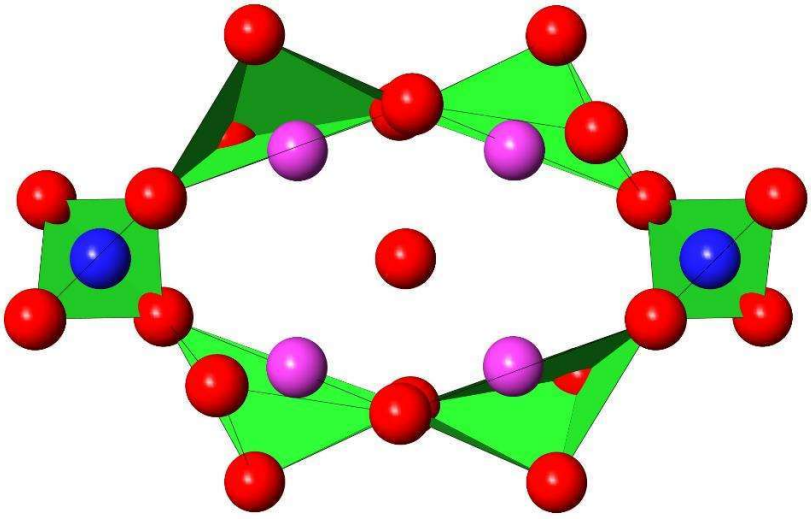

Figure 1.14: The O4 site, in the centre of the diagram [108].

This extra oxygen site is named the O4 site, and is shown in the centre of figure 1.14. Occupation of this site allows more than 20 oxygens to be incorporated into the cell, with an M site charge higher than 4 required to maintain charge balance. An effect of this extra oxygen is to shift the bismuth ions away from the M site tetrahedra slightly. This causes the bismuth co-ordination environment to change to that shown in figure 1.15 where the BiO_4 groups shift from sharing edges to sharing faces, and no longer join to the M site tetrahedra [108].

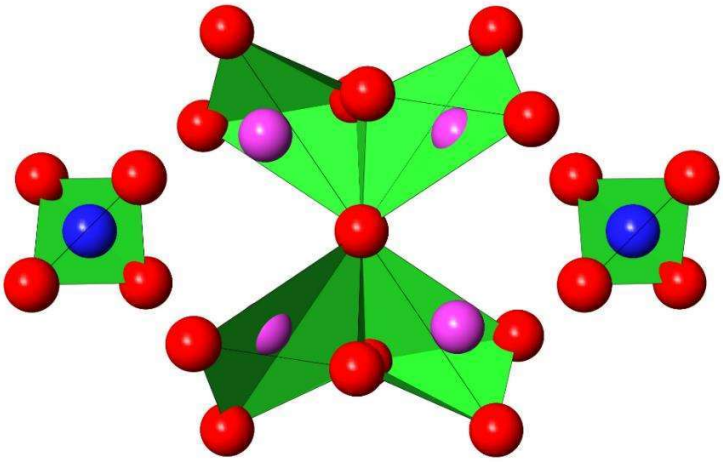

Figure 1.15: The altered bismuth co-ordination environment in an oxygen excess Sillenite [109].

1.13. Applications

Current applications of Sillenites are primarily in the field of electro-optics, where Sillenite single crystals are chosen for the non-linear optical effects they exhibit. Sillenites have a rapid photorefractive response (where refractive index of a material changes when it is illuminated), which makes them suitable for applications in optical processing and holographic data storage . Sillenite crystals are also photoconductive, leading to applications such as interferometry detectors . More recently research on Sillenite ceramics has intensified with interest in future applications as dielectrics.

1.14 Dielectric properties of metal oxide

1.14.1 Capacitors

The capacitor is a component which has the capability (***capacity)*** of stored energy in the form of an electrical charge generates a potential difference across its plates, much like a small rechargeable battery. They are designed to release their energy very quickly. In its basic form, a capacitor consists of two or more parallel conductive plates does not touch each other, but is electrically far either by air or by a good insulating material such as mica, ceramic, plastic waxed paper, and liquid gel as used in electrolytic capacitors. The insulating layer between capacitors plates is known as ***Dielectric***. The potential difference between the conductors, a static electric field develops across the dielectric, due to an alignment of charges in the dielectric. This reason the positive charge to collect on one plate and negative charge on the other plate. The energy of the capacitor is stored in the electrostatic field. The mechanism of working of a parallel plate capacitor in a circuit, including the alignment of charges in the dielectric material is shown in Fig.1.5.

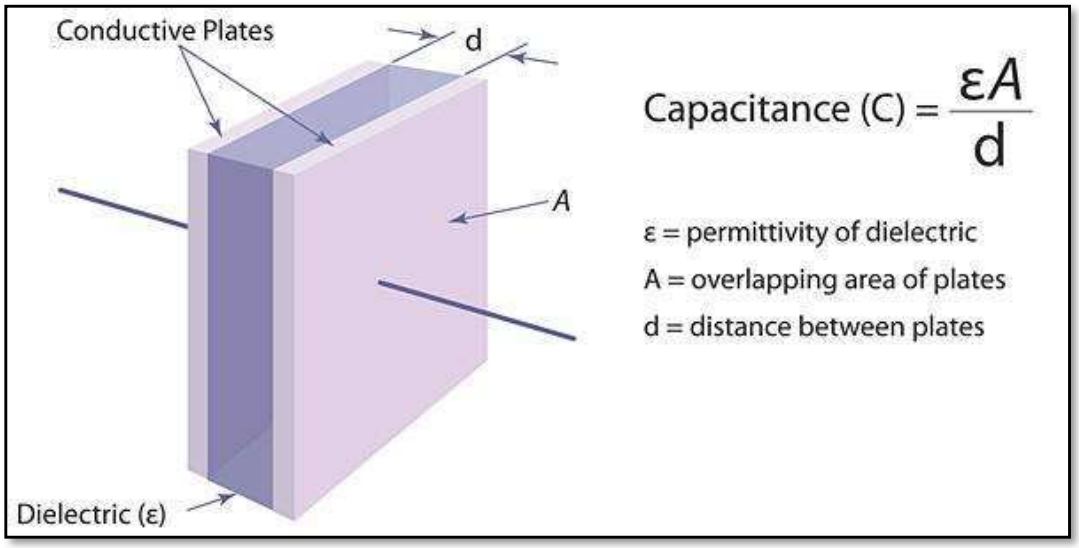

Fig. 1.16. Shows parallel plate capacitors in circuit, including the alignment of charges in the dielectric material [110]

The capacitance of the parallel plate capacitor is shown in the equation:

$$C = \varepsilon_0 A/d \tag{1.1}$$

where, ε_0 (8.854 x 10^{-12} F/m) is the permittivity of free space. The dielectric constant is higher capacitance is also higher which can be realized in a given space. Therefore, materials of the high dielectric constant are favored in the practical design of embedded capacitors for miniaturization.

1.14.2 Dielectric Materials

Ceramic materials described good electrical insulators to as dielectric materials and composite also explain the dielectric and electrical properties. The electric field has applied these type of materials neither observed electrical current or nor inert to the electric field (E). The field reason slightly shifts charge balance in the material as shown in Fig 1.6.

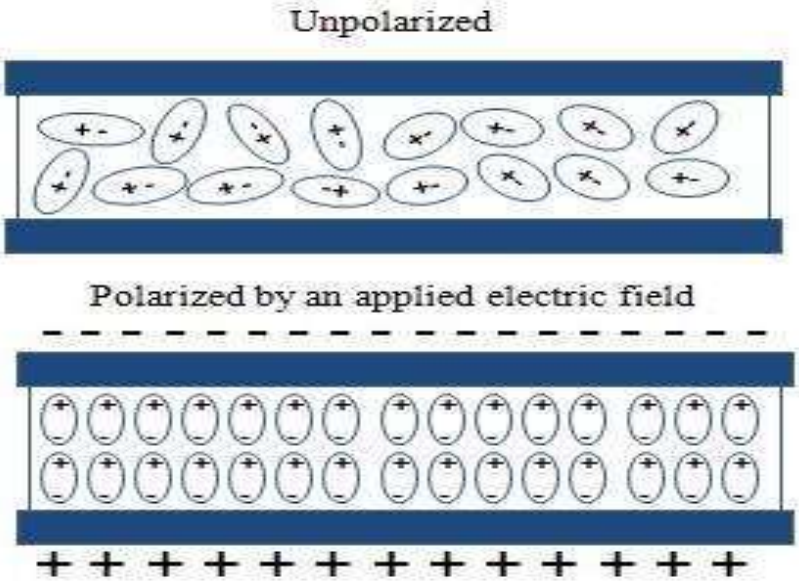

Fig.1.17. The polarized and non-polarized plates of an applied electric field .[111]

So for, the system occupies an electrical dipole moment (P) . These dipole moment found per unit volume is called polarization. The moment is proportional to the electric field (E) and the polarization is proportional to the applied field [112] show in equation

$$P = n\chi eE \tag{1.2}$$

Where, χ_e is the dielectric susceptibility; n is a constant that describes the dielectric ability to form dipoles [113]. Since the dielectric susceptibility χ_e is equal to (ε_{r-1}), where ε_r is the relative permittivity, the polarization will be [114].

$$P = \varepsilon_o E (\varepsilon_{r-1}) \tag{1.3}$$

The field that a molecule in the inward of a dielectric established between the plates of a charged condenser virtually experiences is known to be larger than the applied field. This is related to the polarization which exhibits on the surfaces of the dielectric. The actual field of a molecule is called the local field (E_{loc}). The dipole moment for a molecule by the local field is given by [115].

$$P_{mol} = \alpha' E_{loc} \tag{1.4}$$

where, P_{mol} is a moment and α' shows the polarizability of the molecule. For dielectrics containing N molecules per unit volume, the total dipole moment or polarization is:

$$P = N \alpha' E_{loc} \tag{1.5}$$

Substituting Equation (1.4) in Equation (1.5) gives

$$\chi_e = (\varepsilon_{r-1}) = P/ \varepsilon_o E_{loc} = N \alpha' E_{loc}/ \varepsilon_o E \tag{1.6}$$

The presence of the dielectric material reduces the effective and various polarization mechanisms: Electronic polarization, orientation (dipolar) polarization, space charge

polarization, and atomic or ionic polarization. The net polarization P of the dielectric material, and is given as:

$$P = P_{\text{electronic}} + P_{ionic} + P_{molecular} + P_{interfacial}$$

1.15. Electronic Polarization

Electronic polarization occurs in all dielectric materials. When an electric field (E) acts on an individual atom, the electrons surrounding each nucleus are shifted very slightly in the direction of the positive electrode and the nucleus is very slightly shifted in the direction of the negative electrode and the atom acquires a dipole moment (P), so that:

$$P = \alpha' E \qquad (1.7)$$

As soon as the electric field is removed, the electrons and the nuclei return to their original distributions and polarization disappears. The displacement of charge is very small for electronic polarization, so the total amount of polarization is small compared to the other mechanisms of polarization [116]

1.15.1 Orientation Polarization

If the system is composed of heteronuclear (non-symmetrical) molecules then the disposition of the individual atoms within the molecule may be such that the molecule itself has a permanent dipole moment. Examples are H_2O, HCl, CH_3Br, Hf, and $C_2H_5(NO_2)$. For the H_2O, the covalent bonds between hydrogen and oxygen atoms are directional such that the two hydrogen atoms that have a net positive charge are on one side of the oxygen that has a net negative charge. Under an electric field, the molecule will align with the positive side facing the negative electrode and the negative

side facing the positive electrode[116]. A molecule which is composed of different atoms is not necessarily polar. e.g. CO_2 is non-polar because the carbon and oxygen atoms are arranged in a straight line with the carbon in the middle as shown in table 1.3. H_2O is polar because the ions are arranged in a triangle (table 1.3) [117]. Orientation polarization is better than electronic polarization, because larger charge displacement is possible in the comparatively a large molecules compared to the difference between electrons and nucleus in particular atoms .[116] In solids, however, the molecules are usually too tightly bound for the orientation polarization to occur. It is much more important in liquids and gases. Due to the randomizing effect of the thermal vibrations this type of polarization is more effective as the temperature is decreased and it gives rise to a dielectric constant, which is temperature dependent [117].

1.15.2. Space Charge Polarization

The space charges are random charges caused by cosmic radiation, thermal deterioration, or are trapped in the material during the creation process [116].

1.15.3. Atomic or Ionic Polarization

Atomic polarization involves displacement of atoms (ions) within a crystal structure when an electric field is applied, the field will tend to stretch bonds between the ions and this will change the moment of the molecule. The polarization effects is possible through this mechanism depending on the crystal structure, the presence of solid solution, and other coefficient [116].

Table 1.2. Shows polarization mechanism of dielectric materials

Polarization Mechanism					
Type of polarization	**No E field** (E=0)	**Local Field E** (E≠0)	**Case where it is Observed**	**Frequency range where it is predominant**	**Strength of Polarization**
Electronic Polarization	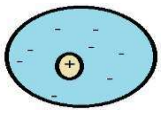	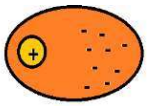	Neutral atoms	~ 10^{15} Hz	Very weak
Atomic or Ionic polarization	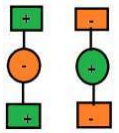	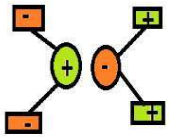	Ionic species	10^{12} to 10^{13} Hz	Strong
Molecular or Orientation or Dipolar Polarization		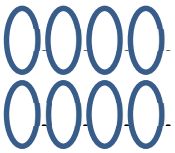	Molecules with permanent dipole moment	10^{11} to 10^{12} Hz	Weak
Interfacial Polarization	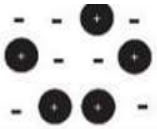	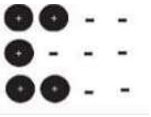	Heterogeneous Systems	10^{-3} to 10^{3} Hz	Very strong

1.11 Dielectric Constant

The charge storage capability and stint of polarization of a material are always define in the term of dielectric constant or as relative permittivity. The electric field is applied to two flat plates of a metal, one plate becomes positive and the other negative. The electric field causes polarization in the material in the space between the conductive plates. The relative dielectric constant (k) compares the polarizability of the material with that of the vacuum between the plates [116].

$$k' = k \text{ Material} / k \text{ vacuum} \quad (1.8)$$

In other references; the relative permittivity is quoted as (ε_r), while, ε_0 is defined as the permittivity of the free space and ε is the permittivity of the dielectric material. The permittivity terms (ε_r, ε_0, ε) will be used according to Equation (1.9).

$$\varepsilon_r = \varepsilon / \varepsilon_0 \quad (1.9)$$

Materials with low dielectric constant are used for electrical insulator applications. Materials with high dielectric constant are used in capacitors for charge storage and other functions. High dielectric constant materials are favored in the design of embedded capacitors to achieve high energy density in a given space and further miniaturization. In an alternating field, dielectric constant (k) can be expressed as

$$k = \varepsilon' - j\varepsilon'' = \varepsilon_0\varepsilon_r - j\varepsilon'' \quad (1.10)$$

where, ε' is real dielectric constant, and ε'' is imaginary dielectric constant. Real dielectric constant (ε') is directly related to the material. Ideally, the dielectric constant should be constant with respect to frequency, temperature, voltage, and time. However, each polarization mechanism has a characteristic relaxation frequency. The values of dielectric materials can also vary with temperature, bias, impurity, and crystal structure by various extents depending on material types[118]

1.16 Dielectric Loss

Dielectric loss is a material property of the dielectric and is a measure of energy loss of the dielectric during ac operation. Dielectric loss is a result of distortion, dipolar,

interfacial and conduction losses. Dielectric loss is expressed as the loss tangent (tan δ) or Dissipation factor (D_f), and is defined as:

$$tan\delta = \varepsilon''\varepsilon' + \sigma 2\pi f\varepsilon \quad (1.11)$$

where, ε', ε'' are real and imaginary parts of dielectric permittivity, σ is electrical conductivity of the material and f is frequency. Energy loss (W) which is defined as the energy dissipated in a dielectric material is proportional to the loss tangent, and is expressed as:

$$W \approx \pi\varepsilon' E2f\ tan\ \delta \quad (1.12)$$

where E is electric field strength and f is frequency. Therefore, a low dielectric loss is preferred in order to reduce the energy dissipation and signal losses, particularly for high frequency applications. Generally, a dissipation factor under 0.1% is considered to be quite low and 5% is high [118]

1.17 Impedance

Impedance spectroscopy is a comparatively good and powerful method for characterizing many of the electrical properties of materials and their interfaces with electronically conducting electrodes. It may investigate the dynamics of bound or mobile charge in the bulk or interfacial regions of any kind of solid or liquid material and always used to ionic, semiconducting, mixed electronic–ionic, dielectrics (even insulators), migration of charge carriers across grain and grain boundaries and other phenomena. Impedance spectroscopy applied a single-frequency voltage or current to the interface and measuring the phase shift and amplitude, or real and imaginary parts, of the resulting current at that frequency using either analog the circuit. The most

important technique is based on analyzing the ac response of a system to a sinusoidal perturbation and consequent calculation of the impedance as a function of the frequency of the perturbation.

Impedance spectroscopy spectrum generally define two categories: (a) the material used itself, such as conductivity, dielectric constant, mobilities of charges, equilibrium concentrations of the charged species, and bulk generation–recombination rates; and (b) an electrode–material interface, such as adsorption–reaction rate constants, capacitance of the interface region and diffusion coefficient of neutral species in the electrode used itself.

It is important and not pied that modern advances in electronic automation have included impedance spectroscopy. Sophisticated automatic experimental equipment has been developed to measure and analyze the frequency response to a small-amplitude ac signal between about 10^{-4} and $>10^{-6}$ Hz, interfacing its results to computers chips, industrial quality control of paints, emulsions, electroplating, thin-film technology, materials fabrication, mechanical performance of engines, corrosion, and so on. The impedance can be represented as a real (Z') and imaginary (Z″) component. Depending on the material and hypothesized process, an electrical equivalent circuit can be constructed made of capacitors, inductors, resistors and other elements. Transforms can be used in order to obtain related values from the impedance. A few transformations are listed below [119].

Table 1.3. High dielectric constant of few oxide compounds

S.No.	Compound	Dielectric constant	Reference
1.	$CaCu_{2.70}Mg_{0.30}Ti_4O_{12}$	3.4×10^5	[120]
2.	$Bi_{2/3}Cu_3Ti_4O_{12}$	2.9×10^4	[121]
3.	$Ba(Fe_{0.5}Nb_{0.5})O_3$-$Bi_{0.2}Y_{2.8}Fe_5O_{12}$	30000	[122]
4.	$Ba_{0.75}Sr_{0.25}TiO_3$	24000	[123]
5.	$CaCu_3Ti_4O_{12}$	20000	[92]
6.	$K_{0.5}Na_{0.5}NbO_3$	20000	[124]
7.	$Bi_{1.5}ZnNb_{1.5}O_7$	10,000	[125]
8.	$0.5BaTiO3–0.5Bi_{2/3}Cu_3Ti_4O_{12}$	43459	[126]
9.	$Ba_6Y_2Ti_4O_{17}$	1.5×10^3	[127]
10.	Eu_2CuO_4	5×10^3	[128]
11.	$0.5Bi_{2/3}Cu_3Ti_4O_{12}$- $0.5Bi_3LaTi_3O_{12}$	13.9×10^3	[121]
12.	$CaCu_{2.9}Zn_{0.1}Ti_4O_{12}$	5971	[120]
13.	$Y_{2/3}Cu_3Ti_{3.95}In_{0.05}O_{12}$	5068	[129]
14	$Bi_{0.5}Na_{0.5}TiO_3$	5000	[130]
15.	$(Ba_{0.95}Ca_{0.05})$ $(Ti_{0.96}Zr_{0.04})O_3$	3910	[131]
16.	$SrTiO_3$	2150	[132]
17.	$Bi_4Ti_3O_{12}$	1400	[128]

The real and imaginary parts of the complex dielectric constant are represented as:

$$\varepsilon' = -Z''/\omega C (Z'^2 + Z''^2) \quad (1.13)$$

$$\varepsilon'' = -Z'/\omega C (Z'^2 + Z''^2) \quad (1.14)$$

The real and imaginary parts of complex electric modulus are represented as:

$$M' = \omega CZ'' \quad (1.15)$$

$$M'' = \omega CZ' \quad (1.16)$$

The loss tangent is given as

$$\tan\delta = \varepsilon'/\varepsilon'' = M''/M' \quad (1.17)$$

the radial frequency, ω, is given as

$$\omega = 2\,\pi\,f \quad (1.18)$$

with f being the frequency and the vacuum capacitance C is given in above (equation 1.1)

$$C = \varepsilon A/d$$

with A is the area of the electrode and d is the thickness of the dielectric layer.

1.18. Adsorption

Adsorption is distinct as the deposition of molecular species onto the surface. The molecular species that gets adsorbed on the surface is known as adsorbate and the surface on which adsorption occurs is known as adsorbent. Common examples of adsorbents are clay, silica gel, colloids, metals etc.[133]

Adsorption is a surface marvel. The process of removal of adsorbent from the surface of adsorbate is known as desorption.

1.18.1. Mechanism of Adsorption

The amount of heat grown when one mole of the adsorbate is adsorbed on adsorbent is called enthalpy of adsorption. Adsorption is an exothermic process and enthalpy change is always negative.[134] When adsorbate molecules are adsorbed on the surface, autonomy of movement of molecules become restricted and this results in decrease in entropy. Adsorption is a natural process at constant pressure and temperature, thus Gibb's free energy is also nigative.

1.18.2 Types of Adsorption

There are two types of Adsorption – Physical Adsorption or Physiosorption and Chemical Adsorption or Chemisorption.

1.18.3 Characteristics of Physical Adsorption

- There is no specificity in case of physical adsorption. Each gas is adsorbed on the surface of the solid.
- Nature of the adsorbate. Easily liquefiable gases are strongly adsorbed physically.
- Physical adsorption is reversible in nature. If pressure is increased volume of gas decreases as a result more gas is adsorbed. So, by decreasing the pressure, gas can be removed from the solid surface. Low temperature promotes physical adsorption and high temperature decreases the rate of adsorption.
- More surface area more is the rate of adsorption. Porous substances and finely divided metals are good adsorbents.
- Physical adsorption is an exothermic process.
- No activation energy is needed.

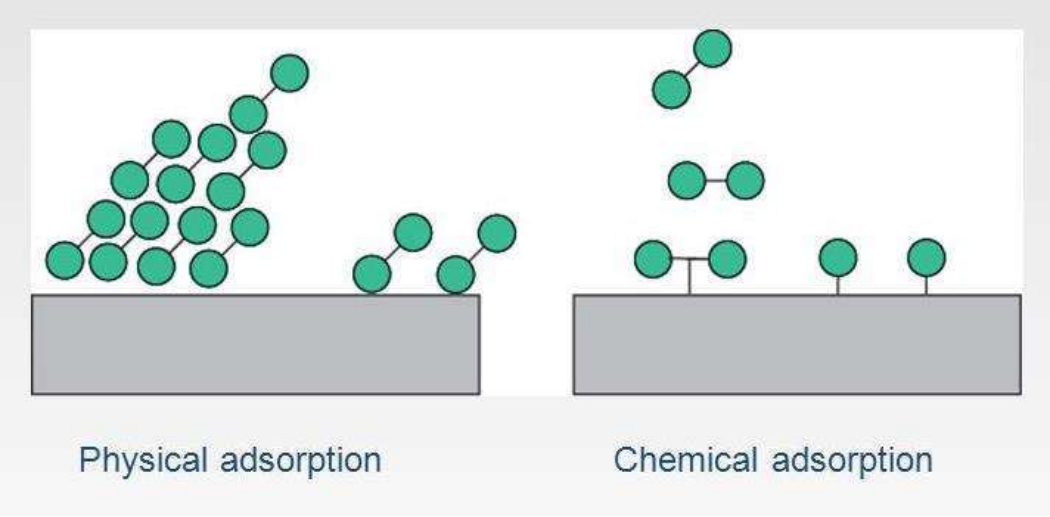

Fig. 1.18. Types of adsorption

1.18.4 Chemical Adsorption or Chemisorption

- When the gas molecules or atoms are detained to the solid surface via chemical bonds, this type of adsorption is chemical adsorption or chemisorption.

Adsorption isotherms

Adsorption isotherm is a graph or a relative between the amounts of adsorbate adsorbed on the surface of adsorbent and pressure at a constant temperature.[135] Different adsorption isotherm was studied by different scientists-

1.18.5. Freundlich Adsorption Isotherm

Freundlich proposed an empirical relationship between amount of gas adsorbed by unit mass of adsorbent and pressure at a particular temperature. Following equation was proposed for freundlich adsorption isotherm.[135]

$$x/m = k.\, p^{1/n}\ (n > 1)$$

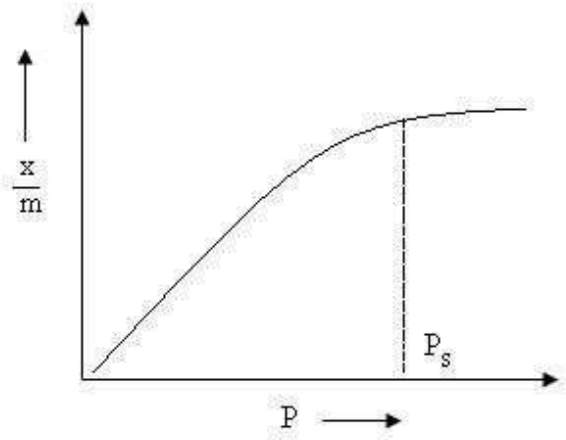

Fig. 1.19. Adsorption isotherm

x is the mass of the gas adsorbed

m is the mass of the adsorbent

p is the pressure

k and n are constants which depends on the nature of the adsorbent and the gas at a particular temperature.

Taking log of the above equation, the following equation will be observed

$$\log x/m = \log k + 1/n \log p$$

x/m is plotted on y axis and log p is on x axis. If straight line is observed than only freundlich isotherm is verified.[135][134]

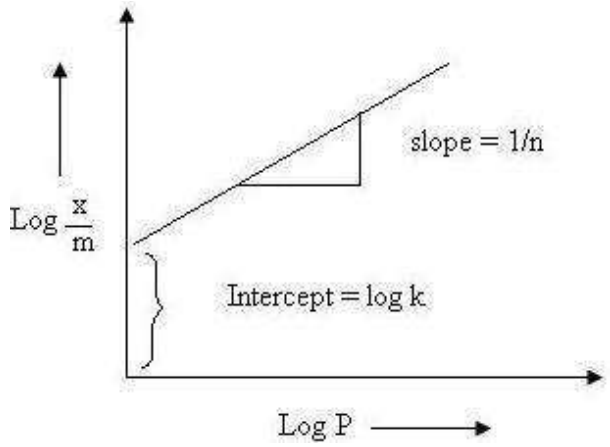

Fig. 1.20. Freundlich isotherm

Slope gives 1/n and intercept gives log k. The value of 1/n varies from 0 to 1.

If 1/n is 0, adsorption is independent of pressure.

If 1/n is 1, adsorption changes with pressure.

References :

[1] M. Halik *et al.*, "Low-voltage organic transistors with an amorphous molecular gate dielectric," *Nature*, vol. 431, no. 7011, pp. 963–966, 2004.

[2] V. H. Grassian, "When size really matters: Size-dependent properties and surface chemistry of metal and metal oxide nanoparticles in gas and liquid phase environments," *Journal of Physical Chemistry C*, vol. 112, no. 47, pp. 18303–18313, 2008.

[3] J. Goniakowski and C. Noguera, "The concept of weak polarity: An application to the SrTiO3(001) surface," *Surface Science*, vol. 365, no. 2, 1996.

[4] M. A. Vest, K. C. Lui, and H. H. Kung, "Catalytic decomposition of methanol on ZnO single-crystal surfaces at low and near-atmospheric pressures," *Journal of Catalysis*, vol. 120, no. 1, pp. 231–255, 1989.

[5] P. Krotee *et al.*, "Atomic structures of fibrillar segments of hIAPP suggest tightly mated β-sheets are important for cytotoxicity," *eLife*, vol. 6, pp. 1–26, 2017.

[6] L. Nakka, J. E. Molinari, and I. E. Wachs, "Surface and bulk aspects of mixed oxide catalytic nanoparticles: Oxidation and dehydration of CH3OH by polyoxometallates," *Journal of the American Chemical Society*, vol. 131, no. 42, pp. 15544–15554, 2009.

[7] A. N. Goldstein, C. M. Echer, and A. P. Alivisatos, "Melting in semiconductor nanocrystals," *Science*, vol. 256, no. 5062, pp. 1425–1427, 1992.

[8] M. A. Reed, W. R. Frensley, R. J. Matyi, J. N. Randall, and A. C. Seabaugh, "Realization of a three-terminal resonant tunneling device: The bipolar quantum resonant tunneling transistor," *Applied Physics Letters*, vol. 54, no. 11, pp. 1034–1036, 1989.

[9] A. P. Alivisatos, "Downloaded from www.sciencemag.org on March 4 , 2011 Downloaded from www.sciencemag.org on March 4 , 2011," *Science*, vol. 271, pp. 933–936, 1996.

[10] F. Raimondi, G. G. Scherer, R. Kötz, and A. Wokaun, "Nanoparticles in energy technology: Examples from electrochemistry and catalysis," *Angewandte Chemie - International Edition*, vol. 44, no. 15, pp. 2190–2209, 2005.

[11] M. Kerker, "Effect of optical constants on calculated values of surface-enhanced Raman scattering," *Journal of the Optical Society of America B*, vol. 2, no. 8, p. 1327, 1985.

[12] M. S. Hassan, T. Amna, H. Y. Kim, and M. S. Khil, "Enhanced bactericidal effect of novel CuO/TiO2 composite nanorods and a mechanism thereof," *Composites Part B: Engineering*, vol. 45, no. 1, pp. 904–910, 2013.

[13] Y. Li, F. Qian, J. Xiang, and C. M. Lieber, "Nanowire electronic and optoelectronic devices," *Materials Today*, vol. 9, no. 10, pp. 18–27, 2006.

[14] G. Wang, X. Shen, J. Yao, and J. Park, "Graphene nanosheets for enhanced lithium storage in lithium ion batteries," *Carbon*, vol. 47, no. 8, pp. 2049–2053, 2009.

[15] R. Xu, "Measuring explained variation in linear mixed effects models," *Statistics in Medicine*, vol. 22, no. 22, pp. 3527–3541, 2003.

[16] A. Yousef *et al.*, "Inactivation of pathogenic Klebsiella pneumoniae by CuO/TiO 2 nanofibers: A multifunctional nanomaterial via one-step electrospinning," *Ceramics International*, vol. 38, no. 6, pp. 4525–4532, 2012.

[17] S. Z. Butler *et al.*, "Progress, challenges, and opportunities in two-dimensional materials beyond graphene," *ACS Nano*, vol. 7, no. 4, pp. 2898–2926, 2013.

[18] O. In, "S Ecurity in W Ireless S Ensor N Etworks," *Ieee Wireless Communications*, vol. 1, no. August, pp. 60–66, 2008.

[19] P. Mani, R. Srivastava, and P. Strasser, "Dealloyed binary PtM3 (M = Cu, Co, Ni) and ternary PtNi 3M (M = Cu, Co, Fe, Cr) electrocatalysts for the oxygen reduction reaction: Performance in polymer electrolyte membrane fuel cells," *Journal of Power Sources*, vol. 196, no. 2, pp. 666–673, 2011.

[20] M. Pudukudy, A. Hetieqa, and Z. Yaakob, "Synthesis, characterization and photocatalytic activity of annealingdependent quasi spherical and capsule like ZnO nanostructures," *Applied Surface Science*, vol. 319, no. 1, pp. 221–229, 2014.

[21] F. S. Ke *et al.*, "One-step fabrication of CuO nanoribbons array electrode and its excellent lithium storage performance," *Electrochimica Acta*, vol. 54, no. 24, pp. 5825–5829, 2009.

[22] H. Pang, F. Gao, and Q. Lu, "Morphology effect on antibacterial activity of cuprous oxide," *Chemical Communications*, no. 9, pp. 1076–1078, 2009.

[23] M. R. Hoffmann, S. T. Martin, W. Choi, and D. W. Bahnemann, "Environmental Applications of Semiconductor Photocatalysis," *Chemical Reviews*, vol. 95, no. 1, pp. 69–96, 1995.

[24] C. Burda, X. Chen, R. Narayanan, and M. A. El-Sayed, *Chemistry and properties of nanocrystals of different shapes*, vol. 105, no. 4. 2005.

[25] T. Hyeon, Su Seong Lee, J. Park, Y. Chung, and Hyon Bin Na, "Synthesis of highly crystalline and monodisperse maghemite nanocrystallites without a size-selection process," *Journal of the American Chemical Society*, vol. 123, no. 51, pp. 12798–12801, 2001.

[26] S. Rana, J. Rawat, M. M. Sorensson, and R. D. K. Misra, "Antimicrobial function of Nd3+-doped anatase titania-coated nickel ferrite composite nanoparticles: A biomaterial system," *Acta Biomaterialia*, vol. 2, no. 4, pp. 421–432, 2006.

[27] M. Pudukudy and Z. Yaakob, "Facile solid state synthesis of ZnO hexagonal nanogranules with excellent photocatalytic activity," *Applied Surface Science*, vol. 292, pp. 520–530, 2014.

[28] P. Sathishkumar, R. Sweena, J. J. Wu, and S. Anandan, "Synthesis of CuO-ZnO nanophotocatalyst for visible light assisted degradation of a textile dye in aqueous solution," *Chemical Engineering Journal*, vol. 171, no. 1, pp. 136–

140, 2011.

[29] T. Yanagimoto, Y. T. Yu, and K. Kaneko, "Microstructure and CO gas sensing property of Au/SnO 2 core-shell structure nanoparticles synthesized by precipitation method and microwave-assisted hydrothermal synthesis method," *Sensors and Actuators, B: Chemical*, vol. 166–167, no. December 2014, pp. 31–35, 2012.

[30] A. Jegatha Christy and M. Umadevi, "Novel combustion method to prepare octahedral NiO nanoparticles and its photocatalytic activity," *Materials Research Bulletin*, vol. 48, no. 10, pp. 4248–4254, 2013.

[31] T. Gordon, B. Perlstein, O. Houbara, I. Felner, E. Banin, and S. Margel, "Synthesis and characterization of zinc/iron oxide composite nanoparticles and their antibacterial properties," *Colloids and Surfaces A: Physicochemical and Engineering Aspects*, vol. 374, no. 1–3, pp. 1–8, 2011.

[32] K. Sieradzka, M. Mazur, D. Wojcieszak, J. Domaradzki, D. Kaczmarek, and E. Prociow, "P-type transparent Ti-V oxides semiconductor thin film as a prospective material for transparent electronics," *Thin Solid Films*, vol. 520, no. 9, pp. 3472–3476, 2012.

[33] J. C. Johnson, H. J. Choi, K. P. Knutsen, R. D. Schaller, P. Yang, and R. J. Saykally, "Single gallium nitride nanowire lasers," *Nature Materials*, vol. 1, no. 2, pp. 106–110, 2002.

[34] L. Kernazhitsky *et al.*, "Optical and photocatalytic properties of titanium-manganese mixed oxides," *Materials Science and Engineering B: Solid-State Materials for Advanced Technology*, vol. 175, no. 1, pp. 48–55, 2010.

[35] A. Aslani, V. Oroojpour, and M. Fallahi, "Sonochemical synthesis, size controlling and gas sensing properties of NiO nanoparticles," *Applied Surface Science*, vol. 257, no. 9, pp. 4056–4061, 2011.

[36] P. Agulhon, V. Markova, M. Robitzer, F. Quignard, and T. Mineva, "Structure of alginate gels: Interaction of diuronate units with divalent cations from

density functional calculations," *Biomacromolecules*, vol. 13, no. 6, pp. 1899–1907, 2012.

[37] L. F. A. Anand Raj, R. Jonisha, B. Revathi, and E. Jayalakshmy, "Preparation and characterization of BSA and chitosan nanopartices for sustainable delivery system for quercetin," *Journal of Applied Pharmaceutical Science*, vol. 5, no. 7, pp. 1–5, 2015.

[38] S. Mahdavi, M. Jalali, and A. Afkhami, "Heavy metals removal from aqueous solutions using tio2, mgo, and al2o3 nanoparticles," *Chemical Engineering Communications*, vol. 200, no. 3, pp. 448–470, 2013.

[39] C. C. Vidyasagar, Y. A. Naik, T. G. Venkatesha, and R. Viswanatha, "Solid-State Synthesis and Effect of Temperature on Optical Properties of CuO Nanoparticles," vol. 4, no. June, pp. 73–77, 2012.

[40] P. Tucci *et al.*, "Metabolic effects of TIO2 nanoparticles, a common component of sunscreens and cosmetics, on human keratinocytes," *Cell Death and Disease*, vol. 4, no. 3, pp. 1–11, 2013.

[41] Y. W. Suh, S. H. Moon, and H. K. Rhee, "Active sites in Cu/ZnO/ZrO2 catalysts for methanol synthesis from CO/H2," *Catalysis Today*, vol. 63, no. 2–4, pp. 447–452, 2000.

[42] C. Wang *et al.*, "Preparation, characterization and photocatalytic activity of nano-sized ZnO/SnO2 coupled photocatalysts," *Applied Catalysis B-Environmental*, vol. 39, pp. 269–279, 2002.

[43] M. Asamoto, S. Miyake, K. Sugihara, and H. Yahiro, "Improvement of Ni/SDC anode by alkaline earth metal oxide addition for direct methane-solid oxide fuel cells," *Electrochemistry Communications*, vol. 11, no. 7, pp. 1508–1511, 2009.

[44] H. J. Snaith and L. Schmidt-Mende, "Advances in liquid-electrolyte and solid-state dye-sensitized solar cells," *Advanced Materials*, vol. 19, no. 20, pp. 3187–3200, 2007.

[45] M. V. B. Zanoni, J. J. Sene, H. Selcuk, and M. A. Anderson, "Photoelectrocatalytic production of active chlorine on nanocrystalline titanium dioxide thin-film electrodes," *Environmental Science and Technology*, vol. 38, no. 11, pp. 3203–3208, 2004.

[46] Q. Yang *et al.*, "Serum retinol binding protein 4 contributes to insulin resistance in obesity and type 2 diabetes," *Nature*, vol. 436, no. 7049, pp. 356–362, 2005.

[47] J. W. Eikelboom, S. R. Mehta, S. S. Anand, C. Xie, K. A. A. Fox, and S. Yusuf, "Adverse impact of bleeding on prognosis in patients with acute coronary syndromes," *Circulation*, vol. 114, no. 8, pp. 774–782, 2006.

[48] D. L. Ge, Y. J. Fan, C. L. Qi, and Z. X. Sun, "Facile synthesis of highly thermostable mesoporous ZnAl2O 4 with adjustable pore size," *Journal of Materials Chemistry A*, vol. 1, no. 5, pp. 1651–1658, 2013.

[49] J. M. Wenzlau *et al.*, "The cation efflux transporter ZnT8 (Slc30A8) is a major autoantigen in human type 1 diabetes," *Proceedings of the National Academy of Sciences of the United States of America*, vol. 104, no. 43, pp. 17040–17045, 2007.

[50] J. Agrell, H. Birgersson, M. Boutonnet, I. Melián-Cabrera, R. M. Navarro, and J. L. G. Fierro, "Production of hydrogen from methanol over Cu/ZnO catalysts promoted by ZrO2 and Al2O3," *Journal of Catalysis*, vol. 219, no. 2, pp. 389–403, 2003.

[51] R. Salomão, M. O. C. V. Bôas, and V. C. Pandolfelli, "Porous alumina-spinel ceramics for high temperature applications," *Ceramics International*, vol. 37, no. 4, pp. 1393–1399, 2011.

[52] C. L. Carnes, J. Stipp, K. J. Klabunde, and J. Bonevich, "Synthesis, characterization, and adsorption studies of nanocrystalline copper oxide and nickel oxide," *Langmuir*, vol. 18, no. 4, pp. 1352–1359, 2002.

[53] A. Zhang *et al.*, "Effect of biochar amendment on yield and methane and

nitrous oxide emissions from a rice paddy from Tai Lake plain, China," *Agriculture, Ecosystems and Environment*, vol. 139, no. 4, pp. 469–475, 2010.

[54] A. Pérez-Larios, R. Lopez, A. Hernández-Gordillo, F. Tzompantzi, R. Gómez, and L. M. Torres-Guerra, "Improved hydrogen production from water splitting using TiO 2-ZnO mixed oxides photocatalysts," *Fuel*, vol. 100, pp. 139–143, 2012.

[55] T. Mahmood, M. T. Saddique, A. Naeem, P. Westerhoff, S. Mustafa, and A. Alum, "Comparison of different methods for the point of zero charge determination of NiO," *Industrial and Engineering Chemistry Research*, vol. 50, no. 17, pp. 10017–10023, 2011.

[56] C. C. Hu, K. H. Chang, M. C. Lin, and Y. T. Wu, "Design and tailoring of the nanotubular arrayed architecture of hydrous RuO2 for next generation supercapacitors," *Nano Letters*, vol. 6, no. 12, pp. 2690–2695, 2006.

[57] R. Terki, G. Bertrand, and H. Aourag, "Full potential investigations of structural and electronic properties of ZrSiO4," *Microelectronic Engineering*, vol. 81, no. 2–4, pp. 514–523, 2005.

[58] P. Goudochnikov and A. J. Bell, "Correlations between transition temperature, tolerance factor and cohesive energy in 2+:4+ perovskites," *Journal of Physics Condensed Matter*, vol. 19, no. 17, 2007.

[59] S. Cabuk, H. Akkus, and A. M. Mamedov, "Electronic and optical properties of KTaO3: Ab initio calculation," *Physica B: Condensed Matter*, vol. 394, no. 1, pp. 81–85, 2007.

[60] M. E. Lines and A. M. Glass, "Primary Pyroelectric Effect in LiTa <math display="inline"> <mrow> <msub> <mrow> <mi mathvariant="normal">O</mi> </mrow> <mrow> <mn>3</mn> </mrow> </msub> </mrow> </math>," *Physical Review Letters*, vol. 39, no. 21, pp. 1362–1365, 1977.

[61] X. N. Yang, N. G. Qu, H. Bin Wang, B. B. Huang, and J. Y. Wei, "A study of

La-doped Bi2Ti2O7 nanocrystals prepared by chemical solution deposition technique," *Materials Letters*, vol. 60, no. 23, pp. 2886–2888, 2006.

[62] M. Bibes and A. Barthélémy, "Oxide spintronics," *IEEE Transactions on Electron Devices*, vol. 54, no. 5, pp. 1003–1023, 2007.

[63] P. K. Davies, H. Wu, A. Y. Borisevich, I. E. Molodetsky, and L. Farber, "Crystal chemistry of complex perovskites: New cation-ordered dielectric oxides," *Annual Review of Materials Research*, vol. 38, pp. 369–401, 2008.

[64] S. Banerjee, D. I. Kim, R. D. Robinson, I. P. Herman, Y. Mao, and S. S. Wong, "Observation of Fano asymmetry in Raman spectra of SrTiO3 and Cax Sr1-xTiO3 perovskite nanocubes," *Applied Physics Letters*, vol. 89, no. 22, pp. 1–4, 2006.

[65] Y. Mao, T. J. Park, and S. S. Wong, "Synthesis of classes of ternary metal oxide nanostructures," *Chemical Communications*, no. 46, pp. 5721–5735, 2005.

[66] Y. Mao, T. J. Park, F. Zhang, H. Zhou, and S. S. Wong, "Environmentally friendly methodologies of nanostructure synthesis," *Small*, vol. 3, no. 7, pp. 1122–1139, 2007.

[67] C. Deng *et al.*, "Synthesis of sillenite-type bi 36 fe 2 o 57 and elemental bismuth with visible-light photocatalytic activity for water treatment," *Frontiers of Materials Science*, vol. 12, no. 4, pp. 415–425, 2018.

[68] D. Seron, C. Collado, J. Mateu, and J. M. O'Callaghan, "Analysis and simulation of distributed nonlinearities in ferroelectrics and superconductors for microwave applications," *IEEE Transactions on Microwave Theory and Techniques*, vol. 54, no. 3, pp. 1154–1159, 2006.

[69] M. Huijben *et al.*, "Electronically coupled complementary interfaces between perovskite band insulators," *Nature Materials*, vol. 5, no. 7, pp. 556–560, 2006.

[70] J. Mateu, J. C. Booth, and B. H. Moeckly, "Nonlinear response of combined superconductor/ferroelectric devices: First experimental step," *IEEE*

Transactions on Applied Superconductivity, vol. 17, no. 2, pp. 942–945, 2007.

[71] C. N. R. Rao, G. U. Kulkarni, P. John Thomas, and P. P. Edwards, "Size-dependent chemistry: Properties of nanocrystals," *Chemistry - A European Journal*, vol. 8, no. 1, pp. 28–35, 2002.

[72] M. Dawber, "I-9 Standar Pembiayaan Pembelajaran FEB," vol. 77, no. October, pp. 1083–1130, 2005.

[73] N. Setter *et al.*, "Ferroelectric thin films: Review of materials, properties, and applications," *Journal of Applied Physics*, vol. 100, no. 5, 2006.

[74] H. Koinuma, "Chemistry and electronics of oxides from carbon dioxide to perovskite," *Thin Solid Films*, vol. 486, no. 1–2, pp. 2–10, 2005.

[75] R. Khenata *et al.*, "First-principle calculations of structural, electronic and optical properties of BaTiO3 and BaZrO3 under hydrostatic pressure," *Solid State Communications*, vol. 136, no. 2, pp. 120–125, 2005.

[76] V. N. Denisov, B. N. Mavrin, V. B. Podobedov, and J. F. Scott, "Hyper-Raman spectra and frequency dependence of soft mode damping in SrTiO3," *Journal of Raman Spectroscopy*, vol. 14, no. 4, pp. 276–283, 1983.

[77] H. Vogt and H. Uwe, "Hyper-Raman scattering from the incipient ferroelectric KTaO3," *Physical Review B*, vol. 29, no. 2, pp. 1030–1034, 1984.

[78] A. S. Hamid, A. Uedono, T. Chikyow, K. Uwe, K. Mochizuki, and S. Kawaminami, "Vacancy-type defects and electronic structure of perovskite-oxide SrTiO 3 from positron annihilation," *Physica Status Solidi (A) Applications and Materials Science*, vol. 203, no. 2, pp. 300–305, 2006.

[79] J. Carrasco *et al.*, "First-principles calculations of the atomic and electronic structure of F centers in the bulk and on the (001) surface of SrTi O3," *Physical Review B - Condensed Matter and Materials Physics*, vol. 73, no. 6, 2006.

[80] E. G. Maksimov, N. L. Matsko, S. V. Ebert, and M. V. Magnitskaya, "Some problems in the theory of perovskite ferroelectrics," *Ferroelectrics*, vol. 354,

no. 1, pp. 19–38, 2007.

[81] D. P. Volanti *et al.*, "Photoluminescent behavior of Sr Bi2 Nb2 O9 powders explained by means of B- Bi2 O3 phase," *Applied Physics Letters*, vol. 90, no. 26, pp. 1–4, 2007.

[82] E. C. Paris *et al.*, "Er3+ as marker for order-disorder determination in the PbTiO3 system," *Chemical Physics*, vol. 335, no. 1, pp. 7–14, 2007.

[83] M. L. Moreira *et al.*, "Photoluminescence of barium titanate and barium zirconate in multilayer disordered thin films at room temperature," *Journal of Physical Chemistry A*, vol. 112, no. 38, pp. 8938–8942, 2008.

[84] A. Z. Simões, C. S. Riccardi, A. Ries, M. A. Ramirez, E. Longo, and J. A. Varela, "Ferroelectric and piezoelectric properties of bismuth layered thin films grown on (1 0 0) Pt electrodes," *Journal of Materials Processing Technology*, vol. 196, no. 1–3, pp. 10–14, 2008.

[85] S. Kato, M. Ogasawara, M. Sugai, and S. Nakata, "Crystal structure and property of perovskite-type oxides containing ion vacancy," *Catalysis Surveys from Asia*, vol. 8, no. 1, pp. 27–34, 2004.

[86] T. Takata *et al.*, "Photocatalytic Decomposition of Water on Spontaneously Hydrated Layered Perovskites," *Chemistry of Materials*, vol. 9, no. 5, pp. 1063–1064, 1997.

[87] K. Domen *et al.*, "A novel series of photocatalysts with an ion-exchangeable layered structure of niobate," *Studies in Surface Science and Catalysis*, vol. 75, no. C, pp. 2159–2162, 1993.

[88] Y. Wang, Y. Zhang, L. Yan, J. Li, C. Wang, and F. Fu, "A novel magnetically recyclable photocatalyst of Bi12TiO20/Co composites with enhanced photocatalytic performance," *Ceramics International*, vol. 43, no. 17, pp. 15965–15969, 2017.

[89] G. H. Jonker, "Semiconducting properties of mixed crystals with perovskite structure," *Physica*, vol. 20, no. 7–12, pp. 1118–1122, 1954.

[90] M. Burisch, "Approaches to personality inventory construction: A comparison of merits," *American Psychologist*, vol. 39, no. 3, pp. 214–227, 1984.

[91] C. J. Ball, B. D. Begg, D. J. Cookson, G. J. Thorogood, and E. R. Vance, "Structures in the System CaTiO3/SrTiO3," *Journal of Solid State Chemistry*, vol. 139, no. 2, pp. 238–247, 1998.

[92] K. Boulahya, D. Muñoz Gil, M. Hassan, S. García Martin, and U. Amador, "Structural and microstructural characterization and properties of new phases in the Nd-Sr-Co-(Fe/Mn)-O system as air-electrodes in SOFCs," *Dalton Transactions*, vol. 46, no. 4, pp. 1283–1289, 2017.

[93] G. Amow, J. Au, and I. Davidson, "Synthesis and characterization of La4Ni3-xCoxO10±δ ($0.0 \leq x \leq 3.0$, $\Delta x = 0.2$) for solid oxide fuel cell cathodes," *Solid State Ionics*, vol. 177, no. 19-25 SPEC. ISS., pp. 1837–1841, 2006.

[94] K. W. Song and K. T. Lee, "Characterization of NdSrCo1-xFexO4+δ ($0 \leq x \leq 1.0$) intergrowth oxide cathode materials for intermediate temperature solid oxide fuel cells," *Ceramics International*, vol. 37, no. 2, pp. 573–577, 2011.

[95] J. Bassat *et al.*, "Anisotropic Oxygen Di ff usion Properties in Pr 2 NiO 4 + δ and Nd 2 NiO 4 + δ Single Crystals," *The Journal of Physical Chemistry C*, 2013.

[96] V. V. Kharton, A. P. Viskup, A. V. Kovalevsky, E. N. Naumovich, and F. M. B. Marques, "Ionic transport in oxygen-hyperstoichiometric phases with K2NiF4-type structure," *Solid State Ionics*, vol. 143, no. 3–4, pp. 337–353, 2001.

[97] X. Li and N. A. Benedek, "Enhancement of ionic transport in complex oxides through soft lattice modes and epitaxial strain," *Chemistry of Materials*, vol. 27, no. 7, pp. 2647–2652, 2015.

[98] F. M. Sapountzi, J. M. Gracia, C. J. (Kee. J. Weststrate, H. O. A. Fredriksson, and J. W. (Hans. Niemantsverdriet, "Electrocatalysts for the generation of hydrogen, oxygen and synthesis gas," *Progress in Energy and Combustion*

Science, vol. 58, pp. 1–35, 2017.

[99] M. N. Popescu, A. Domínguez, W. E. Uspal, M. Tasinkevych, and S. Dietrich, "Comment on 'Which interactions dominate in active colloids?' [J. Chem. Phys. 150, 061102 (2019)]," *The Journal of Chemical Physics*, vol. 151, no. 6, p. 067101, 2019.

[100] M. Dion, M. Ganne, and M. Tournoux, "Nouvelles familles de phases MIMII2Nb3O10 a feuillets 'perovskites,'" *Materials Research Bulletin*, vol. 16, no. 11, pp. 1429–1435, 1981.

[101] J. Liu, C. G. Duan, W. G. Yin, W. N. Mei, R. W. Smith, and J. R. Hardy, "Large dielectric constant and Maxwell-Wagner relaxation in Bi 2/3Cu3Ti4O12," *Physical Review B - Condensed Matter and Materials Physics*, vol. 70, no. 14, 2004.

[102] W. F. Yao *et al.*, "Sillenites materials as novel photocatalysts for methyl orange decomposition," *Chemical Physics Letters*, vol. 377, no. 5–6, pp. 501–506, 2003.

[103] M. Valant and D. Suvorov, "A Stoichiometric Model for Sillenites," pp. 3471–3476, 2002.

[104] M. Valant and D. Suvorov, "A stoichiometric model for sillenites," *Chemistry of Materials*, vol. 14, no. 8, pp. 3471–3476, 2002.

[105] M. Valant and D. Suvorov, "A stoichiometric model for sillenites," *Chemistry of Materials*, vol. 14, no. 8, pp. 3471–3476, 2002.

[106] D. C. Craig and N. C. Stephenson, "Structural studies of some body-centered cubic phases of mixed oxides involving Bi2O3: The structures of Bi25FeO40 and Bi38ZnO60," *Journal of Solid State Chemistry*, vol. 15, no. 1, pp. 1–8, 1975.

[107] B. M. O. M. Si, "Processing and Dielectric Properties of Sillenite Compounds Bi12MO20-δ.pdf," vol. 904, pp. 2900–2904, 2001.

[108] M. Ru, V. N. Kanepit, A. N. Yudin, and A. A. Mar, "Math-Net.Ru," 2021.

[109] M. Ru, V. I. Simonov, and V. A. Sarin, "Math-Net.Ru," vol. 306, no. 3, pp. 624–627, 2021.

[110] M. Jackson, A. Collins, D. Berlowitz, M. Howard, F. O'Donoghue, and M. Barnes, "Efficacy of sleep position modification to treat positional obstructive sleep apnea," *Sleep Medicine*, vol. 16, no. 4, pp. 545–552, 2015.

[111] C. Wang, B. Hawlader, and D. Perret, "Finite Element Simulation of the 2010 Saint-Jude Landslide in Quebec," *Proceedings 16th CGS Conference Geovancouver - History And Innovation*, no. February 2017, pp. 1–8, 2016.

[112] Y. Jun *et al.*, "Effects of Nb-doping on electric and magnetic properties in multi-ferroic BiFeO 3 ceramics," vol. 135, pp. 133–137, 2005.

[113] J. Hsia *et al.*, "Calcium/vitamin D supplementation and cardiovascular events," *Circulation*, vol. 115, no. 7, pp. 846–854, 2007.

[114] A. E. Nogueira, E. Longo, E. R. Leite, and E. R. Camargo, "Visible-light photocatalysis with bismuth titanate (Bi 12 TiO 20) particles synthesized by the oxidant peroxide method (OPM)," *Ceramics International*, vol. 41, no. 9, pp. 12073–12080, 2015.

[115] D. Voll, A. Beran, and H. Schneider, "Variation of infrared absorption spectra in the system Bi2 Al4-xFexO9 (x=0-4), structurally related to mullite," *Physics and Chemistry of Minerals*, vol. 33, no. 8–9, pp. 623–628, 2006.

[116] K. I. Osman, "Synthesis and Characterization of BaTiO3 Ferroelectric Material," *UniMAP*, p. 176, 2011.

[117] J. Sólyom, *Fundamentals of the physics of solids*, vol. 3. 2010.

[118] D. Mannath, L. W. Schaper, and R. K. Ulrich, "Advanced decoupling in high performance IC packaging," *Proceedings - Electronic Components and Technology Conference*, vol. 1, pp. 266–270, 2004.

[119] Y. K. V. Reddy, D. Mergel, and W. Osswald, "Impedance spectroscopy study

of RuO2/SrTiO3 thin film capacitors prepared by radio-frequency magnetron sputtering," *Materials Science and Engineering B: Solid-State Materials for Advanced Technology*, vol. 130, no. 1–3, pp. 237–245, 2006.

[120] L. Singh, U. S. Rai, K. D. Mandal, and A. K. Rai, "Effect of processing routes on microstructure, electrical and dielectric behavior of Mg-doped CaCu3Ti4O12 electro-ceramic," *Applied Physics A: Materials Science and Processing*, vol. 112, no. 4, pp. 891–900, 2013.

[121] P. Gautam, S. S. Yadava, A. Khare, and K. D. Mandal, "Dielectric and magnetic studies of 0.5Bi2/3Cu3Ti4O12 - 0.5Bi3LaTi3O12 nano-composite ceramic synthesized by semi-wet route," *Ceramics International*, vol. 43, no. 3, pp. 3133–3139, 2017.

[122] L. Yang, X. Chao, P. Liang, L. Wei, and Z. Yang, "Electrical properties and high-temperature dielectric relaxation behaviors of NaxBi(2-x)/3Cu3Ti4O12 ceramics," *Materials Research Bulletin*, vol. 64, pp. 216–222, 2015.

[123] "Perovskite oxide having general formula ABO 3 has been widely investigated because of their excellent electrical, dielectric, optoelectronic and piezoelectric properties. The properties of the perovskite can be modified by a variety of partial substitutio," no. Mlcc.

[124] Y. B. Pottathara *et al.*, "Mechanically strong, flexible and thermally stable graphene oxide/nanocellulosic films with enhanced dielectric properties," *RSC Advances*, vol. 6, no. 54, pp. 49138–49149, 2016.

[125] M. George, S. S. Nair, K. A. Malini, P. A. Joy, and M. R. Anantharaman, "Finite size effects on the electrical properties of sol-gel synthesized CoFe2O4 powders: Deviation from Maxwell-Wagner theory and evidence of surface polarization effects," *Journal of Physics D: Applied Physics*, vol. 40, no. 6, pp. 1593–1602, 2007.

[126] A. Khare, S. S. Yadava, K. D. Mandal, and N. K. Mukhopadhyay, "Effect of sintering duration on the dielectric properties of 0.9BaTiO3–0.1CaCu3Ti4O12 nanocomposite synthesized by solid state route," *Microelectronic Engineering*,

vol. 164, no. 3, pp. 1–6, 2016.

[127] S. S. Yadava, L. Singh, S. Sharma, K. D. Mandal, and N. B. Singh, "Effect of temperature on the dielectric and ferroelectric properties of a nanocrystalline hexagonal Ba4YMn3O11.5-: δ ceramic synthesized by a chemical route," *RSC Advances*, vol. 6, no. 72, pp. 68247–68253, 2016.

[128] P. Salame, R. Drai, O. Prakash, and A. R. Kulkarni, "IBLC effect leading to colossal dielectric constant in layered structured Eu2CuO4 ceramic," *Ceramics International*, vol. 40, no. 3, pp. 4491–4498, 2014.

[129] L. Singh, I. W. Kim, B. C. Sin, A. Ullah, S. K. Woo, and Y. Lee, "Study of dielectric, AC-impedance, modulus properties of 0.5Bi0.5Na0.5TiO3·0.5CaCu3Ti4O12 nano-composite synthesized by a modified solid state method," *Materials Science in Semiconductor Processing*, vol. 31, pp. 386–396, 2015.

[130] P. Lunkenheimer, R. Fichtl, S. G. Ebbinghaus, and A. Loidl, "Nonintrinsic origin of the colossal dielectric constants in CaCu 3Ti4O12," *Physical Review B - Condensed Matter and Materials Physics*, vol. 70, no. 17, pp. 1–4, 2004.

[131] L. Yang, X. Chao, Z. Yang, N. Zhao, L. Wei, and Z. Yang, "Dielectric constant versus voltage and non-Ohmic characteristics of Bi2/3Cu3Ti4O12 ceramics prepared by different methods," *Ceramics International*, vol. 42, no. 2, pp. 2526–2533, 2016.

[132] Y. Xiang, A. Tong, P. Jin, and Y. Ju, "New fluorescent rhodamine hydrazone chemosensor for Cu(II) with high selectivity and sensitivity," *Organic Letters*, vol. 8, no. 13, pp. 2863–2866, 2006.

[133] M. A. Rauf, S. B. Bukallah, F. A. Hamour, and A. S. Nasir, "Adsorption of dyes from aqueous solutions onto sand and their kinetic behavior," *Chemical Engineering Journal*, vol. 137, no. 2, pp. 238–243, 2008.

[134] K. He *et al.*, "Graphene hybridized polydopamine-kaolin composite as effective adsorbent for methylene blue removal," *Composites Part B:*

Engineering, vol. 161, no. October 2018, pp. 141–149, 2019.

[135] M. K. Verma *et al.*, "Bi25feo40 polycrystalline ceramic as highly efficient photocatalyst synthesised via economical chemical route," *Materials Technology*, vol. 35, no. 8, pp. 483–493, 2020.